RBS-MLP: A Machine Learning Approach for Detecting Rogue Base Stations in 5G Mobile Networks

Mohammad Saedi[a], Adrian Moore[b], Philip Perry[b], Chunbo Luo[c], Raj Muttukrishnan[a]

[a]*Department of Computer Science, City, University of London, Northampton Square, London, EC1V OHB, UK*
[b]*School of Computing, Ulster University, York Street, Belfast, BT15 1AP, UK*
[c]*Department of Computer Science, University of Exeter, Northampton Square, Exeter, EX4 4RN, UK*

Abstract

The 3GPP Security Group has identified the detection of Rogue Base Stations (RBS) in 5G networks as one of the leading security challenges for users and network infrastructure. Motivated by this, RBS-MLP, a novel deep learning model, has been developed to identify RBSs. The model uses signal strength measurements in each mobile device's periodic measurement reports as input data, a reliable metric readily available to the system. We investigate the impacts of various sizes of datasets, different window sizes of received signal strength, and different proportional splits of the dataset into training and test data to evaluate the performance of the proposed model. We further demonstrate RBS-MLP using a realistic dataset of received signal strength measurements for a vehicle driving along various sections of a road, providing a use case to demonstrate the use of RBS-MLP to improve the safety of mobile networks. Experimental results reveal that RBS-MLP is well suited as a 99.999% accuracy classification model and provides a new baseline method for RBS detection.

Keywords:
Rogue Base Station (RBS), 5G Mobile Networks, Attack Detection, Vehicle Platooning, Machine Learning (ML), Received Signal Strength (RSS), Measurement Report (MR), gNodeB.

1. Introduction

Rogue Base Stations (RBS) are wireless devices that impersonate a legitimate Base Station (BS), causing subscribers within a certain radius to connect to those devices rather than genuine networks. An RBS attack can happen during the initial cell search stage in the 5G NR when a User Equipment (UE) looks for a suitable BS to camp on. During this stage, the UE listens to the wireless broadcast channel for the synchronising signal (SS) from nearby BSs. Next, the UE selects a BS based on the received SSs and initiates a wireless connection. If an RBS broadcasts a spoofing SS with high Received Signal Strength (RSS) during the cell search mechanism, the UE may be enticed to it and try to camp on it rather than any legitimate BSLi et al. (2021). In the emerging 5G world, it will be vital for infrastructure providers to protect against such attacks to secure the communications platform and protect client data and identity.

Since the inception of early GSM networks, RBS attacks have continuously evolved and persisted. These can be categorised as Denial of Service (DoS) attacks on mobile devices or networks, provision of fraudulent services, and compromising of subscribers' privacy. The impact of these attacks varies greatly among cellular network generations but remains significant owing to the multiple interconnections across a diverse set of current and legacy networksNakarmi et al. (2021). The development of 5G communications has already led to some advancements in RBS detection, such as Subscription Permanent Identifier (SUPI) concealment, guaranteed Globally Unique Temporary Identity (GUTI) refreshment, and protected redirections. At the same time, other security mechanisms inherited from previous generations include mutual authentication between UE and network, secure algorithm negotiations, and integrity-protected signallingAlrashede and Shaikh (2019). Despite these advances, the current position is that 5G remains vulnerable to RBS attack 3GPP Technical Report 33.809 (2023).

Most current RBS detection systems implement a data-gathering capability in the UE, which then either (i) performs analysis on the data gathered at UE-side, or (ii) sends the collected data to a central server for cloud-side detection, or (iii) to the wider network for analysis known as network-based detectionAIMSICD; SRLabs; Li et al. (2017); Steig et al. (2016). Of these, the first group is prone to false positives because a UE cannot understand the complete status of the network view at any given time, and in addition, UE-side detection systems often need software updates on the device or root privileges, which are uncommon and may be difficult for some users. In the second group, the devices send their Measurement Reports (MR) to a central server in the 5G Core for analysis; otherwise, they operate on the same premise as UE-side detectors and, as a result, suffer from the same efficacy and scalability concerns.

Email addresses: mohammad.saedi@city.ac.uk (Mohammad Saedi), aa.moore@ulster.ac.uk (Adrian Moore), p.perry@ulster.ac.uk (Philip Perry), c.luo@exeter.ac.uk (Chunbo Luo), R.muttukrishnan@city.ac.uk (Raj Muttukrishnan)

The third group, Network-based detection systems, are projected to perform better in terms of analysis since, unlike UEs, mobile networks have knowledge of the system's global status. However, a supporting monitoring infrastructure to collect data from multiple network locations or protocols is required. We focus on the third group, which is more applicable to 5G and cellular systems.

In recent years, there has been a lot of interest in Machine Learning (ML) for detecting security threats. ML models can identify security assaults by learning the behaviour of both attack and legitimate scenarios. ML-based classification systems can provide high levels of precision in the identification of potential aggressors Chulerttiyawong and Jamalipour (2023); Dey et al. (2023). We use supervised classification methods to detect attacks in 5G vehicular platooning Saedi et al. (2022). This paper presents the design, implementation, and development of an RBS detection system named RBS-MLP, exploring ML methods to detect RBS in 5G networks effectively. The proposed approach is essentially based on MR filtering. We present a case study demonstrating RBS detection in a realistic dataset of radio information and Received Signal Strength (RSS) measurements generated by a simulation of a vehicle travelling along various road sections.

RBS-MLP is aimed to protect IoT devices by filtering RBS from MR to detect all rogue agents with as few false positives as possible, without specialised hardware. In summary, this research study provides the following contributions:

- Providing a 3GPP Release 18 compliant RBS detection model. The device-assisted part of the model uses the standard measurement reporting procedure, while the network-based part performs the data analysis using a deep learning RBS detection system.
- Evaluating the performance of the RBS-MLP algorithm in terms of the accuracy of classification between rogue and legitimate BS.
- Proposing an enhanced handover protocol to include a BS trust mechanism to evaluate the trustworthiness of the BS.
- Using the ML approach in a simulation of a platoon moving along sections of roads containing a mix of legitimate and rogue base stations.

The rest of the paper is structured as follows. In Section 2, we review the related research in RBS detection systems while identifying their limitations. Section 3 presents a novel RBS detection model comprising a pre-processing component and a decision maker. Section 4 proposes the RBS-MLP model. Section 5 presents the performance evaluation and results for various case studies based on our realistic dataset of radio information and RSS measurements taken by a simulated vehicle travelling along various sections of a road. Finally, the conclusions and future works are discussed in Section 6.

2. Related Work

In this section, we report a summary of existing RBS detection systems, mentioned in the previous section, according to the techniques used. In addition, drawbacks and some limitations will be described here.

The UE-side includes client-side applications that perform the identification within the UEs. This includes mobile phones, vehicles, IoT devices, etc. Android IMSI-Catcher Detector (AIMSICD)AIMSICD, Cell Spy CatcherCell Spy Catcher (Anti Spy), CatcherCatcher CatcherCatcher, and SnoopSnitchSRLabs are some applications that fall into this group. To provide some level of protection, these apps require high privileges and low-level access to baseband chips to reach their full potential. Even though Cell Spy Catcher and AIMSICD results have not been persuasive, Cell Spy Catcher at least can be used to determine if the local network figures have been modified. SnoopSnitch seems to be the most advanced of the alternatives, as it reliably informs the user immediately after the threat is detected. In contrast, Cell Spy Catcher only provides a warning and associated information. SnoopSnitch, on the other hand, only works on Qualcomm-based Android phones and requires root access. Similarly, CatcherCatcher attempts to detect RBS activity by detecting irregularities in mobile networks, but it only works on Osmocom phones. To summarise, these apps are still in the early stages of development for detecting RBS attacks. They have a lower detection rate, generate more false positives, and require unusually high-level access, making them unsuitable for the general publicBrenninkmeijer (2016).

Techniques for cloud-based detection are based on analysing the crowdsourced data from a nearby massive number of UEs to detect and geolocate RBS units. FBS-RadarLi et al. (2017), a large-scale RBS detection and localisation system, identifies an RBS through the automated collection of suspicious SMS messages from end-user devices. In addition, these reports, including Received Signal Strength (RSS), cell identifier and UE MAC addresses, are sent to a server to analyse and evaluate different techniques that exploit this data to identify RBS installations accurately without analysing the content of the SMS messages. Van Do et al. Van Do et al. (2015) suggested a methodology for detecting abnormal behaviour from an RBS in public data sets using ML approaches. InDo et al. (2016), the experiment was extended using machine learning and exploiting a signature-based strategy with characteristics such as location and the relationship between the identification number of the UE and subscription. These investigations used a publicly available data set from AftenpostenAftenposten (2015) to demonstrate the utility of ML approaches, but with the drawback that UEs must report their measurements to a server on the cloud for analysis; otherwise, they operate like a client-side detector. As a result, they suffer from effectiveness and scalability issues.

Network-based detection techniques conduct the analysis on the core of the cellular network. InSteig et al. (2016), a technique for IMSI catcher detection has been proposed that uses existing operational data from the mobile network used in the mobility management of mobile stations. The MRs delivered by the UEs to BSs containing information on the cell and surrounding cells are used to detect IMSI catchers. Regarding analysis, network-based detection systems are projected to outperform client-side detectors since mobile networks know the

system's global status, unlike UEs. However, a limitation with Steig et al. (2016) is that they only cover 2G radio access technology. MuratNakarmi et al. (2021) is a network-based approach for recognising RBSs on several 3GPP Radio Access Technologies (RAT) without changing mobile phones or monitoring equipment. Murat employs the global state to include information on all connected mobile phones, the mobile network state, and its deployment and setup history. It outperforms earlier systems.

Traditional RBS techniques are purposefully planned, making it difficult for networks to adjust dynamically. ML is the process of self-learning from experiences and deeds and such approaches can be used to respond appropriately in such situations without human intervention or reprogramming. Deep learning, a subset of machine learning, has grown in popularity in recent years and has been used for RBS detectionDong et al. (2016); studies have shown that deep learning outperforms previous approachesYin et al. (2017). Recent advancements in machine learning models for rogue base station detection include the development of frameworks like FBSDetector, which utilises real-world datasets for detecting multi-step attacks and fake base stations with high accuracyMubasshir et al. (2024).

3. Proposed Detection Model for Rogue Base Stations

In this section, first, the framework of the detection model is proposed. Then a novel handover protocol will provide a key feature for the ML method to build the main component of the RBS detection system.

The analyser component of the RBS-MLP is an ML-based approach based on MR; it can be considered an additional feature for Murat Nakarmi et al. (2021). Murat offers a network-based approach for identifying bogus base stations that run on any 3GPP radio access technology without needing to modify mobile phones. However, the analyser of Murat consists of data processors and Rule-based methods; we analyse the MR using ML methodsNakarmi and Norrman (2018); 3GPP TS 33.501 (2024).

3.1. Proposed Architecture for RBS detection

Fig. 1 describes the proposed architecture to model an RBS identification system to detect rogue agents using machine learning methods. The UE in RRC_CONNECTED mode builds the MR based on signals received from gNBs currently in range and sends it to the 5G Radio Access Network (RAN). The proposed system performs the data analysis, identifies suspected RBS and eliminates them from consideration for handover3GPP TR 38.300 (2024). As a result, the suspected RBS is never included in the version of the MR used to assess the need for a handover event. The BS identifies the need for a handover and, if required, initiates the protocol. Upon detection of an RBS, the network operators can be informed so that legal action and other post-incident activities can be initiated. For example, they can alarm the UE from camping on the RBSGorrepati et al. (2021); Component, D. H. S. and Callahan (2019).

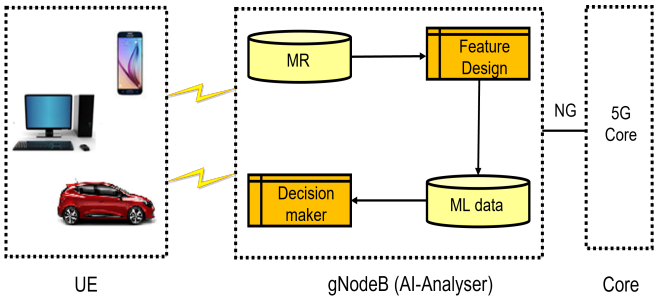

Figure 1: RBS detector Architecture, illustrating the flow of MR from UE to the 5G RAN for analysis and classification using AI.

Such analysers might be included in either the 5G RAN or the 5G Core, however, in this work, the integration of the analysis into the 5G RAN is examined. This decision can be explained by the need for scalability, which is most readily done when the RBS detector is situated at the point where the gNodeB receives the MR dataNakarmi and Norrman (2018).

Fig. 1 illustrates the components of the AI Analyser, comprising a Feature Design element, an AI-based Decision-maker element, and two MR and ML data storage units. The aim of Feature Design is to create informative and relevant input features that help the model distinguish between the two classes. The ML approaches will be used in the decision-making function. The Decision Maker, as the significant component of the AI Analyser, will receive the ML data and apply the ML method to identify rogues. Other Analyser functions can employ various strategies for classification, but we will demonstrate the effectiveness of an ML approach. The sections that follow expand on the architecture's description and details.

3.2. Handover Process

In a 5G environment, an IoT device typically has a selection of BS units within its reception range and the way the device decides which BS to attach is based on an analysis of the device's MR. The MR identifies the most vital received BS signals from the current location and orientation and is updated periodically, usually every second. Depending on the received signal strength of the currently connected BS and the signal strengths of alternate candidate BS units, the device will be told by the network either to stay with the current BS or handover to a more robust alternative. Handover management is critical for ensuring that UEs may move freely between cells while still receiving high-quality communication services. The gNB is in charge of managing UE migration across cells. Typically the handover decision in 5G RAN is based on the MR produced by UEsShaik et al. (2018). The handover process is that the UE is currently connected to a gNB (the serving BS); if there is another BS in the MR with a level that exceeds the threshold value, then we handover to it. Fig. 2 illustrates the Received Signal Strength (RSS) from a collection of 30 BS encountered by a platoon leader along a stretch of urban motorway. As the UE moves along the highway, the handover process is activated, resulting in the connected signal strength profile illustrated in Fig. 3.

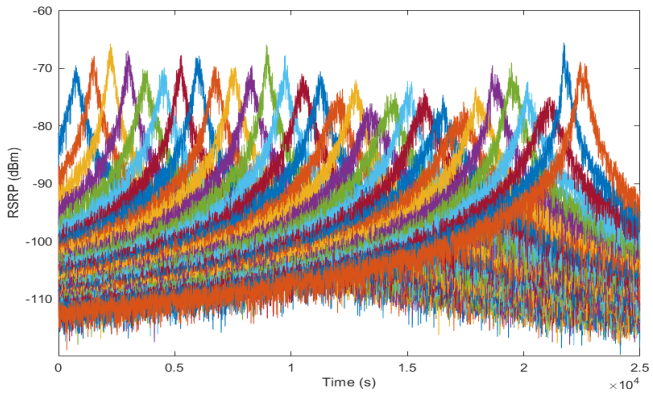

Figure 2: RSS of base stations encountered by a vehicle along a highway in a legitimate scenario.

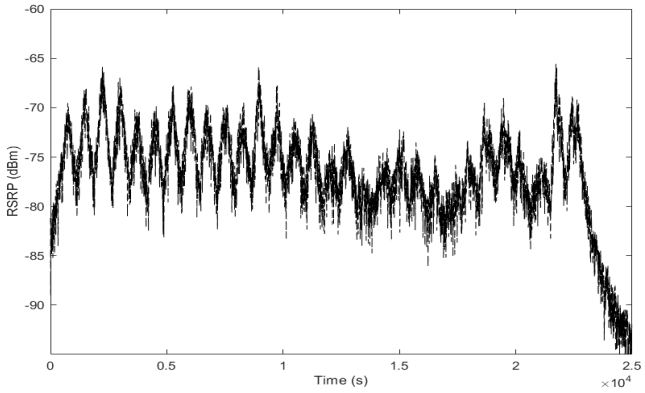

Figure 3: Handover decision-making process based on RSS in a legitimate scenario, demonstrating smooth transitions between base stations.

3.3. Feature Design for RBS Detection

To entice surrounding UEs, an RBS often transmits higher-than-normal signal power. A steep increase and fall in RSS is a characteristic of the profile of a typical rogueSaedi et al. (2022), which can be used as a fingerprint for detection. Therefore, this section defines and implements two new features including the Rate of Change (RoCH) and Probation Period. These informative features are calculated and monitored for all BS and RBS that UE detects. The main idea is that the RoCH is a better indicator for RBS detection than ”raw” RSS data, as RBS tend to increase at a more rapid rate than ”regular” BS. Following is a description of the Probation period.

Fig. 4, for instance, demonstrates BS1, the connected BS, with decreasing power over time as BS2 rises. The RoCH of BS2 can be collected if its readings during the Probation Period are monitored. The Probation Period begins when the BS is first detected and concludes when sufficient consecutive MR values have been recorded. The optimal number of values will be determined later in the following sections. In the diagram, the timestamp ”C” indicates the beginning of the Probation Period or Candidate BS Monitoring Period, and the timestamp ”H” indicates the transition time.

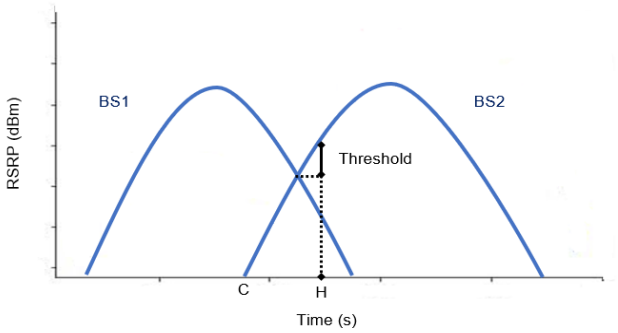

Figure 4: Monitoring period of a candidate base station, showing signal strength transition and rate of change evaluation.

The analysis is a continuous procedure that proceeds regardless of any handover. The RBS (in red) in Fig. 5 is recognized as a rogue before the probable handover point. The next sections will describe various possibilities depending on whether both BS and rogue could be in the MR at the same time or not. However, a rogue agent must not be taken into account for handover.

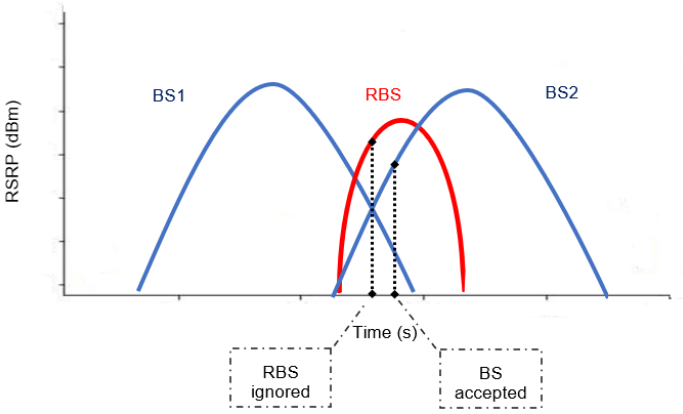

Figure 5: Detection of a rogue base station before handover, ensuring exclusion from the process.

The BS Analysis system will use RoCH as one of its essential features to learn any fingerprint related to the RBS. In addition, it will be considered in the ML approach by constructing a fingerprint of the rogue data stream and attempting to identify what is in a dataset that characterises it as legitimate or rogue.

3.4. Proposed Analysis System

By analyzing the RSS value ranges, it can be observed that the MR’s strongest signal values are around -70 and -75, while the weakest signals are around -90 and -95. These values are influenced by the distance between the BS and the road and the power of the BS transmission. The graph in Fig. 6 shows an attack scenario where RBS values increase and decrease more rapidly compared to LBS values. Consequently, the average

rate of RoCH for RBS is significantly higher during the initial rise period than for LBS. As the RoCH is dependent on the speed of the vehicle, the system needs to learn and adjust the threshold accordingly.

Fig. 7 demonstrates the transfer to RBS in this particular scenario. The timeframes when the platoon leader is linked to an LBS are denoted by a blue signal, while the connection to an RBS is indicated by a red signal.

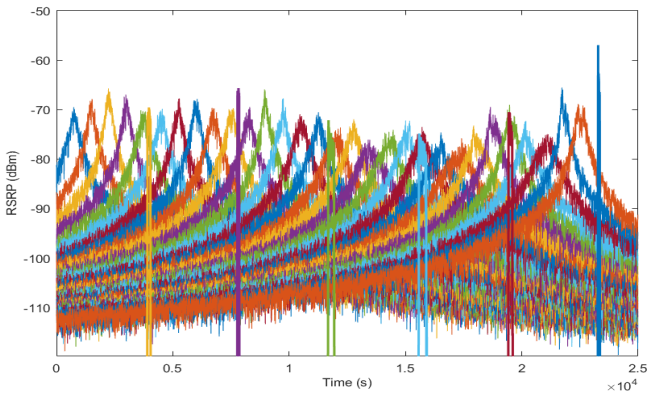

Figure 6: Attack scenario showing rapid RBS signal changes compared to LBS, used for RBS detection.

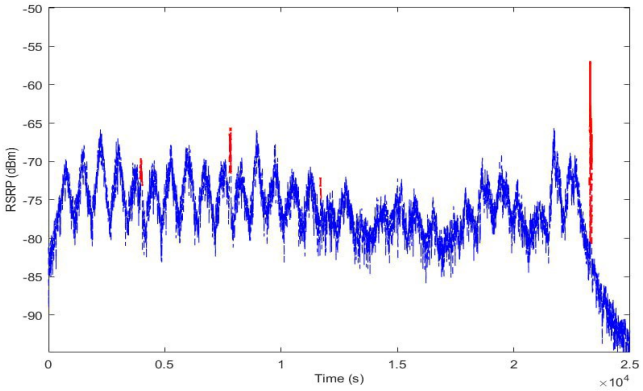

Figure 7: Handover decision-making in an attack scenario, showing the transition between legitimate and rogue base stations.

This research introduces a novel BS monitoring model that takes into account the potential presence of rogue actors in the mobile network. According to this proposal, which is depicted in Fig. 8, a state machine is designed with three states for each BS, including a blocked state that is reserved for a BS that has been identified as a rogue in the MR and should not be considered for handover:

- Blocked state: a BS that will not be considered for handover. This may be because it has been assessed as potentially rogue by the classifier, or because it has been recently discovered and not yet completed its probation period.
- Candidate state: a BS that has completed its probation period and has not exhibited any rogue-like characteristics. If the RSS of a candidate BS exceeds that of the currently connected BS, then a handover event is initiated.
- Connected state: the currently "active" BS. Only one BS will be in this state at any time.

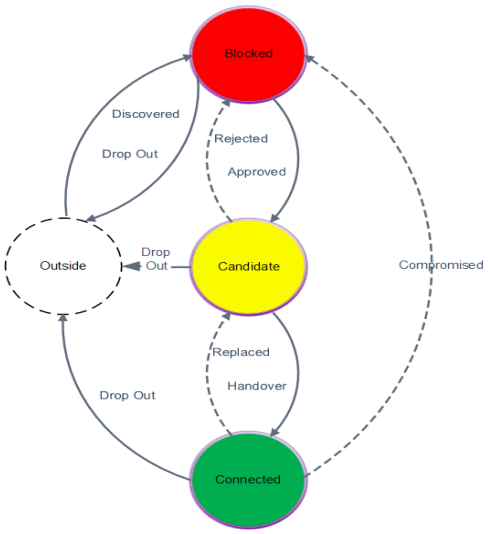

Figure 8: State machine for base stations, illustrating transitions between blocked, candidate, and connected states.

A newly discovered BS should be blocked until the probation period has expired. Upon completion of the probationary period, the BS will be approved. Each BS moves between the states depending on the rate of change of its signal strength. For example, a candidate exhibits a sudden large jump in its RSS value resulting in it being classified as a rogue and becoming blocked (Rejected). Alternatively, if a candidate rises normally and becomes the strongest signal exceeding the handover threshold, then it will be the subject of a handover event and will become connected (handover). If the currently connected BS is no longer the strongest, it will be replaced and revert to the candidate state (replaced), or the connected BS might exhibit rogue-like behaviour so would be immediately blocked. The Drop Out arc from other states to the "Outside" state machine represents a BS that drops out of the MR. In reality, it needs to move out of range and then be rediscovered and pass a probation period to become a candidate. A "Discovered" BS cannot become a candidate until it has been observed and checked for a complete window of timestamps. During this period, it is in the Blocked state. The aim is to remove the arcs connecting "Candidate" and "Connected" with "Blocked" by detecting RBS before they are considered for detection.

4. The AI Analyser for the RBS Detection

This section intends to investigate the effectiveness of the ML method in distinguishing between rogue and legitimate signals by training it with both types of instances. The aim is to eliminate the need for a predetermined threshold level in the process.

4.1. Measurement Report Generation

The 3GPP Technical Report 38.33138.331 (2024) outlines UE measurement reports that contain pertinent data to identify Rogue Base Stations (RBS). The reports include the cell identity and Received Signal Strength (RSS), as well as information about cell groups (CGI_info) that incorporate data from both the MIB and SIB1.

The simulation tool utilised in the research can simulate a vast number of BS and RBS along an extensive motorway, as discussed in Saedi et al. (2020). However, not all data related to BS and RBS can be accessed by the handover mechanism simultaneously. According to the 3GPP specification, the MR component stores only the six strongest Received Signal Strength (RSS) values at any given time van Thanhe et al. (2015); Barco et al. (2001), which are calculated based on the received signals from the six most prominent BS within the platoon leader's vicinity, as depicted in Fig. 9.

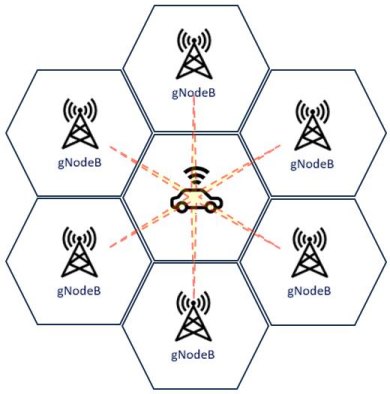

Figure 9: Multiple data streams represent BSs, but only a maximum of six BSs is included in MR at any time.

4.2. The ML Dataset Generation

When a new BS is discovered, it is assigned the "Blocked" state. Once it has been present in the MR for a defined number of consecutive samples, it can be analysed to determine whether it is legitimate ("Candidate") or rogue ("Blocked"). Therefore, it is the first run of consecutive values that should be used as training data for the proposed model and the optimal length of this initial run is determined in the following sections.

The Feature Design component in Fig. 1 takes the accumulated MR data over a simulation period and generates the ML dataset which will be utilised specifically for training the ML classifier. In addition, the rate of changes can be added as well to have more features for learning more to identify RBS accurately.

The experiments carried out in this study necessitate using a dataset that contains both malicious and legitimate BSs. The simulations include different road lengths and BS/RBS positions/densities Saedi et al. (2022). When the UE (in this scenario, the lead vehicle of a platoon) is within the range of the BSs, the received signal is calculated per second.

A snapshot of the ML training data, which includes data streams from both LBS and RBS, is shown in Table 1. Each BS is assigned its own line in the data, with the first set of consecutive RSS readings for that BS in the MR and an identification (L for LBS, R for RBS) following.

The width of the sample window is the quantity of RSS samples included in each BS set. Alternative window sizes will be looked into even though the size of the window in this example is assumed to be 10.

Three datasets of different sizes have been created as described in Table 2. For example, in the first dataset, we simulate a 500 km road with 30000 timestamps in which there are 90 legitimate BSs and 18 rogue BSs. The details of the three datasets are presented.

Table 2: Simulation parameters for datasets used in RBS detection, detailing the number of base stations, road length (Km), and timestamps (S)

Dataset	LBS	RBS	Road Length	TS
90LBS–18RBS	90	18	500	30000
500LBS–90RBS	500	90	4000	170000
1000LBS–180RBS	1000	180	5000	225000

4.3. Classification Model for RBS Detection

The classification stage in Machine Learning is a procedure for determining whether or not an observation falls into a specific category. Here, it detects whether an unknown base station (observation) is genuine or fake (categories).

This section will demonstrate how datasets and features were combined to generate classifier models to correctly identify a stream of received signal values as representing either a legitimate or rogue BS. The classifier is trained by feeding it successive data streams (one stream at a time), indicating for each whether the stream represents a legitimate or rogue BS.

Once the classifier has learned how to differentiate between legitimate and rogue streams, we can then pass it an unknown stream representing the output from either a legitimate or rogue BS and have it classified.

An artificial neural network algorithm is implemented to verify the model performance. The detection model proposed is a binary classification Multilayer Perceptron (MLP) using the sequential API as shown in Fig. 10. The classifier includes three hidden layers. The first layer consists of "relu" activation function with a 'he_normal' weight initialisation to overcome the problem of vanishing gradients when training deep neural network models. The activation functions in the second layer are the "tanh" and "sigmoid" functions. The optimiser is "SGD" (Stochastic Gradient Descent), and the loss function is "binary_crossentropy". The selection of all activation functions and loss functions was based on the analysis results.

5. PERFORMANCE EVALUATION AND RESULTS

In this stage, we will apply our classifier to test data sets to evaluate the accuracy and reliability of our method. First, we

Table 1: Example of ML training dataset for RBS detection, showing consecutive Received Signal Strength (RSS) values for legitimate (L) and rogue (R) base stations

BS(i)	Timestamp(i)										BS Target
	RSS1	RSS2	RSS3	RSS4	RSS5	RSS6	RSS7	RSS8	RSS9	RSS10	
BS(1)	-76.601	-76.545	-76.426	-75.997	-75.659	-75.418	-75.334	-75.154	-75.040	-75.583	L
BS(2)	-82.753	-81.928	-81.835	-81.686	-80.905	-82.026	-82.161	-81.919	-81.874	-81.666	L
BS(3)	-84.585	-84.817	-85.761	-85.991	-86.332	-86.516	-86.462	-86.439	-85.777	-85.655	L
BS(4)	-87.612	-88.044	-87.889	-86.993	-87.592	-87.623	-88.213	-87.058	-87.102	-87.290	L
BS(5)	-90.285	-89.245	-89.290	-89.188	-88.509	-87.579	-87.804	-88.252	-87.731	-87.887	L
BS(6)	-90.862	-90.232	-90.018	-89.431	-89.628	-88.791	-90.088	-89.592	-89.791	-89.952	L
BS(7)	-89.820	-89.463	-89.647	-89.154	-69.260	-68.773	-65.956	-66.554	-65.613	-66.044	L
BS(i-1)	-79.483	-74.951	-69.992	-69.564	-69.679	-70.132	-69.947	-69.899	-71.056	-70.889	R
BS(i)	-83.950	-80.313	-75.188	-70.416	-70.399	-70.267	-70.876	-70.851	-70.891	-71.973	R
BS(n-1)	-84.039	-79.276	-75.123	-75.509	-74.913	-75.110	-75.424	-75.446	-75.697	-76.000	R
BS(n)	-92.281	-87.595	-83.476	-78.500	-74.190	-74.293	-74.622	-74.371	-74.691	-75.132	R

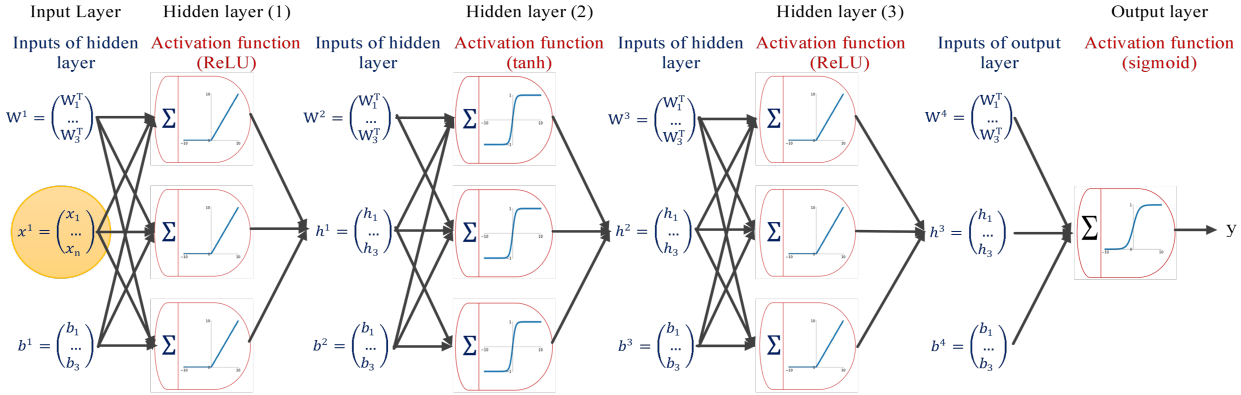

Figure 10: Artificial neural network architecture used for rogue base station detection, featuring multiple hidden layers for classification.

will consider some evaluation metrics in the following paragraph and then show some diagrams to show and compare the results with the following scenarios.

- True positive (TP): positive samples correctly classified as positive, here, i.e., correctly identified LBS. This would remain in the ”Candidate” or ”Connected” state in the state machine provided in Section 3.
- True negative (TN): negative samples correctly classified as negative, i.e., correctly identified RBS; refer to a state diagram in which BS would move into (or remain in) the “Blocked” state.
- False-positive (FP): negative samples incorrectly classified as positive, here, i.e., wrongly identified LBS; BS which should be “blocked” remains as “candidate”. When an RBS has been identified as a legitimate (FP), it makes a critical situation in the handover process – a situation that we are trying to prevent.
- False-negative (FN): positive samples correctly classified as negative, i.e., wrongly identified RBS; In this case, the BS which is a legitimate “candidate” is wrongly “blocked”. Not the desired outcome, but not a disaster as long as we are currently connected, or another legitimate candidate is available. Therefore, when a legitimate BS is identified as a rogue, the impact is less significant.

Four different metrics are used for each classifier’s evaluationSelis and Marshall (2018), Gyawali et al. (2020). First, accuracy is the classifier’s ability to categorise the samples: Accuracy = (TP+TN)/(TP+TN+FP+FN) Second, Recall or Sensitivity, is the proportion of positive samples that are classed as positive. It is also called Sensitivity or True Positive Rate (TPR), which is the LBS detection probability: Recall = TP/(TP+FN). Third, Precision is the proportion of correct positive classifications (TP) from cases predicted as positive: Precision = TP/(TP+FP). Fourth, the F1-score is the harmonic mean and takes precision and recall into account: F1-score = 2*(Precision*Recall)/(Precision+Recall).

Next, we examine the model’s performance and investigate the effects of different data set sizes, RSS window sizes, and different portions of training and test data sources. Through experimentation, we compared three datasets with 70/30 splits between training and testing as well as varied window widths of RSS in terms of accuracy, recall, precision, and F1-score.

As might be predicted, accuracy may be observed to grow as more data is taken into account. A 70/30 split between training and testing data results in an accuracy result of 0.975 for WS=3 with 500 LBS and 90 RBS, as indicated in Fig. 11 by a dashed green line.

The green line indicates that this metric increases to 0.985 with an 80/20 split between training and testing data. Accuracy rises even further for the bigger dataset, hitting 0.995 for the 500LBS-90RBS dataset and 0.99999 for the 1000LBS-180RBS dataset. Similarly, the precision, recall, and F1-score metrics will rise with larger datasets and training data, which will be explored in the following part.

The greater the window size, the more data there will be to work with to make a more accurate conclusion. The Accuracy measure in Fig. 11 shows that WS=3 is not a sufficiently trustworthy size, and so it is not an adequate size for a window. WS=5 is substantially more reliable, although WS=7 yields 0.995 accuracy. However, for the biggest dataset, WS=10 is the best choice overall, with accuracy=0.99999.

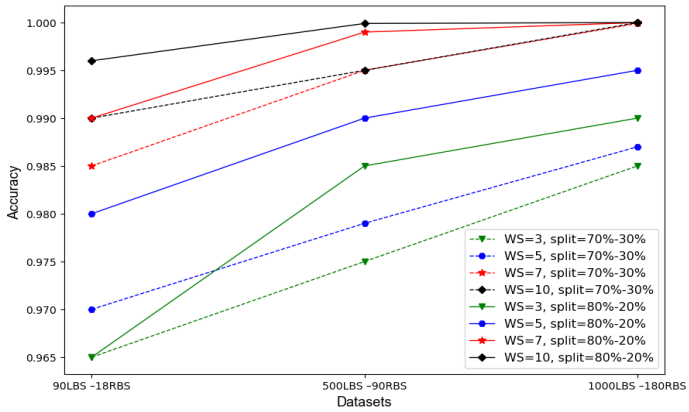

Figure 11: Accuracy comparison of classification models across different RSS window sizes, demonstrating the performance improvement with larger datasets and optimised window selection.

However, when it comes to the overhead of using a bigger window size than is necessary, it is more likely that a larger window may hamper connection since a possible BS will be blocked for a longer amount of time, which may result in latency. Blocking a BS from handover for a longer length of time owing to a wider window may have a detrimental influence on signal availability to the platoon.

The decision-making process becomes more accurate as the range of possibilities widens. Nevertheless, even after exploring WS=12 and WS=15, it was found that they did not yield better results than WS=10. Consequently, the experiment was terminated at WS=10, and now WS=10 can be fully trusted. There is no justification to consider larger window lengths at this point. Fig. 12, Fig. 13 and Fig. 14 show the findings for the other three performance metrics, revealing that the precision, F1-score, and recall factors for the 90LBS-18RBS dataset are 0.997, 0.998, and 1.0, respectively, and improve with larger comprehensive datasets.

Table 3 demonstrates that the True Negative Rate (TNR),

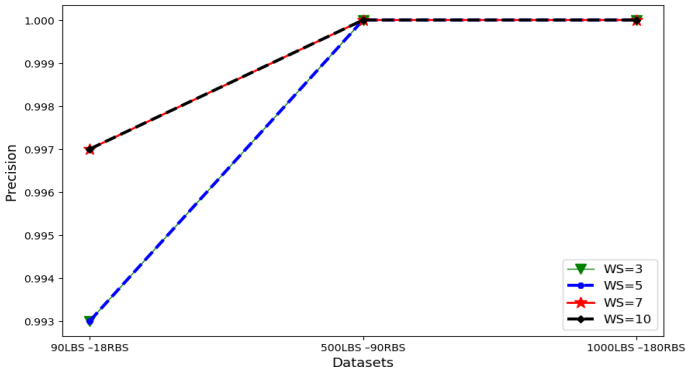

Figure 12: Precision metrics across different RSS window sizes, showing the model's accuracy in identifying legitimate base stations.

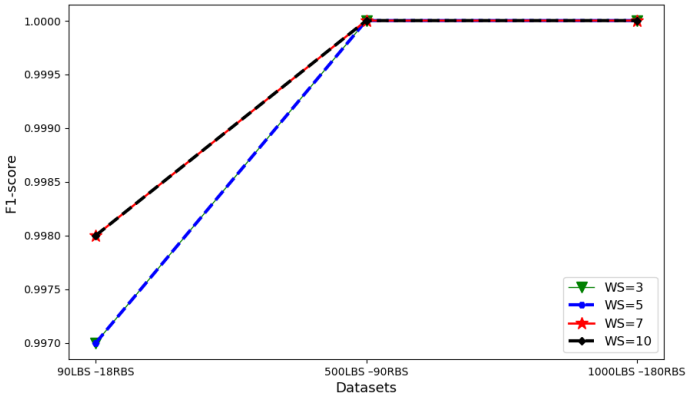

Figure 13: F1-score comparison across varying dataset sizes and RSS window lengths, reflecting the balance between precision and recall.

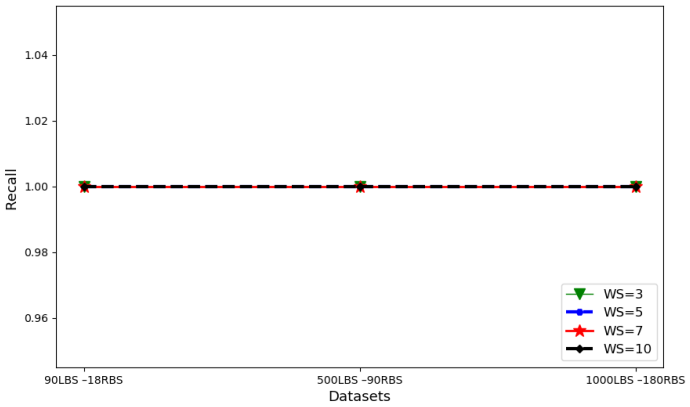

Figure 14: Recall metrics for different RSS window sizes, indicating the model's sensitivity in detecting rogue base stations.

varies between 98.97% and 100% for various datasets with varying divisions of training and test data, implying that the detection probability of RBS for the proposed model is about 99.50%. On the other hand, the maximum bound of the False Positive Rate (FPR) that detects rogue agents as genuine is around 1%. The 500LBS-90RBS dataset appears to be an anomaly, outperforming the 1000LBS-180RBS dataset. Moreover, the False Negative Rate (FNR), which measures the probability that LBS is a rogue, is also zero.

In general, when the dataset is much smaller, there is less training data available, resulting in FP. Except for 500LBS-90RBS, all datasets attain an FPR close to zero. Plotting the loss function rate is a helpful technique to see if the model is appropriately trained. During model training, the loss function is utilised to determine the target value for the model will achieve. We have used binary cross-entropy from the Keras library, a high-level neural network library, in our experiment. It is used in binary classification model as a loss function and computes the difference in cross-entropy between true and predicted labels. This is crucial to ensuring that the model is fitted correctly. Fig. 15 shows the loss rate of the model for the same configuration. The minimal rate is accomplished in a variety of datasets. The results reveal that the loss rate is unaffected by window size; nevertheless, the larger the dataset, the lower the loss rateIan et al. (2017); Reed and MarksII (1999).

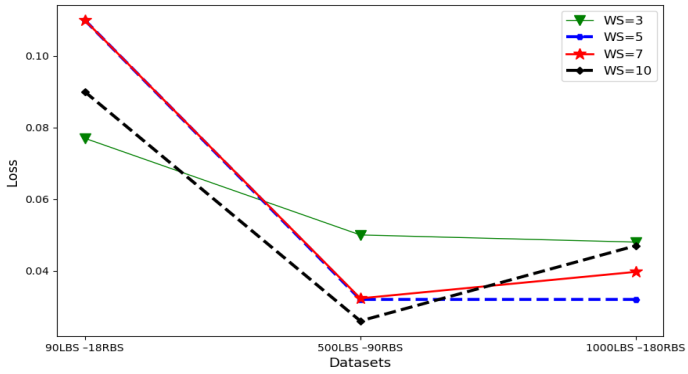

Figure 15: Training loss rate for varying dataset sizes, demonstrating the model's convergence during the learning process.

6. CONCLUSION AND FUTURE WORK

5G includes many measures to help secure the network and protect users' privacy and security. However, one of the most pressing issues in user and network security, as recognised by the 3GPP Security Group, is the identification of malicious agents in mobile networks. RBS attacks have been identified as a significant threat. So, the detection of RBS attacks will be a substantial contribution to knowledge from this research. We have designed and implemented a new method to intelligently detect the presence of a rogue by using a Multi-Layer Perceptron technique. The system is termed RBS-MLP and it is 3GPP compliant. The system can be deployed in the gNBs of a 5G RAN to gather information from Measurement Reports from mobile devices and analyse how the reported signal strength varies with time to identify a signal from an RBS. We have tested this system with large sets of synthetic data from a vehicle platooning scenario to fine tune the system. The results show that the ML approach produces 99.999% accuracy, i.e., is one misclassification in every 100,000, with some specific results and provides a new baseline method for RBS detection. Also, will help to improve 5G services in our target deployment (platooning). The next step of the work will involve the deployment of various AI/ML techniques and comparing performance metrics. Moreover, using real-world datasets like the FBSDetector system could provide enhanced accuracy for rogue base station detection Mubasshir et al. (2024). Another promising approach involves the use of xApps for rogue base station detection in SDR-enabled O-RAN systems, which leverage software-defined radios to enhance detection accuracy in 5G networksHuang et al. (2023).

acknowledgments

This research has been supported by the BT Ireland Innovation Centre (BTIIC) project, funded by BT, and Invest Northern Ireland.

References

38.331, G.T.S., 2024. Radio resource control (rrc) protocol specification. 3rd Generation Partnership Project .

3GPP Technical Report 33.809, 2023. Study on 5G Security Enhancement against False Base Stations (FBS). 3rd Generation Partnership Project .

3GPP TR 38.300, 2024. NR and NG-RAN Overall Description. 3rd Generation Partnership Project .

3GPP TS 33.501, 2024. Security architecture and procedures for 5G system. 3rd Generation Partnership Project .

Aftenposten, 2015. Aftenposten public data set. URL: https://www.aftenposten.no/meninger/kommentar/i/9mrn5/derfor-publiserer-aftenposten-hele-datagrunnlaget-for-mobilspionasje-s. accessed on 2023-01-05.

AIMSICD, . Android imsi-catcher detector. URL: https://github.com/CellularPrivacy/Android-IMSI-Catcher-Detector. accessed on 2022-11-20.

Alrashede, H., Shaikh, R.A., 2019. IMSI Catcher Detection Method for Cellular Networks. 2nd International Conference on Computer Applications and Information Security, ICCAIS 2019 , 1–6doi:10.1109/CAIS.2019.8769507.

Barco, R., Cañete, F.J., Diez, L., Ferrer, R., Wille, V., 2001. Analysis of mobile measurement-based interference matrices in gsm networks. IEEE Vehicular Technology Conference 3, 1412–1416. doi:10.1109/VTC.2001.956429.

Brenninkmeijer, B., 2016. Catching imsi-catcher-catchers: An effectiveness review of imsi-catcher-catcher applications. Bachelor Thesis, Radboud University (Nijmegen, The Netherlands) .

CatcherCatcher, . Mobile network assessment tools. URL: https://opensource.srlabs.de/projects/mobile-network-assessment-tools/wiki/CatcherCatcher. accessed on 2023-01-03.

Cell Spy Catcher (Anti Spy), . Skibapps. URL: https://play.google.com/store/apps/details?id=com.skibapps.cellspycatcher. accessed on 2022-15-12.

Chulerttiyawong, D., Jamalipour, A., 2023. Sybil attack detection in internet of flying things-ioft: A machine learning approach. IEEE Internet of Things Journal 10, 12854–12866. doi:10.1109/JIOT.2023.3257848.

Component, D. H. S. and Callahan, 2019. Privacy Impact Assessment, (U.S. Department of Homeland Security. URL: https://www.dhs.gov/xlibrary/assets/privacy/privacy{_}pia{_}template.pdf.

Dey, M.R., Patra, M., Mishra, P., 2023. Efficient detection and localization of dos attacks in heterogeneous vehicular networks. IEEE Transactions on Vehicular Technology .

Table 3: Performance metrics for RBS detection, including True Positive Rate (TPR), True Negative Rate (TNR), False Positive Rate (FPR), and False Negative Rate (FNR) across various dataset sizes and window settings

	FPR				FNR			
Dataset	WS=3	WS=5	WS=7	WS=10	WS=3	WS=5	WS=7	WS=10
90LBS–18RBS	0	0	0	0	0	0	0	0
500LBS–90RBS	1.03	1.03	1.03	1.03	0	0	0	0
1000LBS–180RBS	0	0	0	0	0	0	0	0

	TPR				TNR			
Dataset	WS=3	WS=5	WS=7	WS=10	WS=3	WS=5	WS=7	WS=10
90LBS–18RBS	100	100	100	100	100	100	100	100
500LBS–90RBS	100	100	100	100	98.97	98.97	98.97	98.97
1000LBS–180RBS	100	100	100	100	100	100	100	100

Do, V.T., Engelstad, P., Feng, B., van Do, T., 2016. Strengthening mobile network security using machine learning, in: Mobile Web and Intelligent Information Systems: 13th International Conference, MobiWIS 2016, Vienna, Austria, August 22-24, 2016, Proceedings 13, Springer. pp. 173–183.

Dong, Z., Kane, K., Camp, L.J., 2016. Detection of rogue certificates from trusted certificate authorities using deep neural networks. ACM Transactions on Privacy and Security (TOPS) 19, 1–31.

Gorrepati, U., Zavarsky, P., Ruhl, R., 2021. Privacy protection in lte and 5g networks, in: 2021 2nd International Conference on Secure Cyber Computing and Communications (ICSCCC), IEEE. pp. 382–387.

Gyawali, S., Qian, Y., Hu, R.Q., 2020. Machine learning and reputation based misbehavior detection in vehicular communication networks. IEEE Transactions on Vehicular Technology 69, 8871–8885.

Huang, J.H., Cheng, S.M., Kaliski, R., Hung, C.F., 2023. Developing xapps for rogue base station detection in sdr-enabled o-ran, in: IEEE INFOCOM 2023-IEEE Conference on Computer Communications Workshops (INFOCOM WKSHPS), IEEE. pp. 1–6.

Ian, G., Yoshua, B., Aaron, C., 2017. Deep learning: Adaptive computation and machine learning.

Li, X., Garcia-Saavedra, A., Costa-Perez, X., Bernardos, C.J., Guimarães, C., Antevski, K., Mangues-Bafalluy, J., Baranda, J., Zeydan, E., Corujo, D., et al., 2021. 5growth: An end-to-end service platform for automated deployment and management of vertical services over 5g networks. IEEE Communications Magazine 59, 84–90.

Li, Z., Wang, W., Wilson, C., Chen, J., Qian, C., Jung, T., Zhang, L., Liu, K., Li, X., Liu, Y., 2017. Fbs-radar: Uncovering fake base stations at scale in the wild. Internet Society doi:10.14722/ndss.2017.23098.

Mubasshir, K.S., Karim, I., Bertino, E., 2024. Fbsdetector: Fake base station and multi step attack detection in cellular networks using machine learning. URL: https://arxiv.org/abs/2401.04958, arXiv:2401.04958.

Nakarmi, P.K., Ersoy, M.A., Soykan, E.U., Norrman, K., 2021. Murat: Multi-rat false base station detector. arXiv preprint arXiv:2102.08780 .

Nakarmi, P.K., Norrman, K., 2018. Detecting false base stations in mobile networks. URL: https://www.ericsson.com/en/blog/2018/6/detecting-false-base-stations-in-mobile-networks.

Reed, R., MarksII, R.J., 1999. Neural smithing: supervised learning in feedforward artificial neural networks. Mit Press.

Saedi, M., Moore, A., Perry, P., 2022. Synthetic generation of realistic signal strength data to enable 5g rogue base station investigation in vehicular platooning. Applied Sciences 12, 12516.

Saedi, M., Moore, A., Perry, P., Shojafar, M., Ullah, H., Synnott, J., Brown, R., Herwono, I., 2020. Generation of realistic signal strength measurements for a 5g rogue base station attack scenario, in: 2020 IEEE Conference on Communications and Network Security (CNS), pp. 1–7. doi:10.1109/CNS48642.2020.9162275.

Selis, V., Marshall, A., 2018. A classification-based algorithm to detect forged embedded machines in iot environments. IEEE Systems Journal 13, 389–399.

Shaik, A., Borgaonkar, R., Park, S., Seifert, J.P., 2018. On the impact of rogue base stations in 4g/lte self organizing networks, in: Proceedings of the 11th ACM Conference on Security & Privacy in Wireless and Mobile Networks, pp. 75–86.

SRLabs, . Snoopsnitch, imsi catcher score. URL: https://opensource.srlabs.de/projects/snoopsnitch/wiki/IMSI_Catcher_Score. accessed on 2023-01-05.

Steig, S., Aarnes, A., Van Do, T., Nguyen, H.T., 2016. A network based imsi catcher detection, in: 2016 6th International Conference on IT Convergence and Security (ICITCS), IEEE. pp. 1–6.

van Thanhe, D., Jørstad, I., van Thuan, D., 2015. Strong authentication for web services with mobile universal identity, in: Mobile Web and Intelligent Information Systems: 12th International Conference, MobiWis 2015, Rome, Italy, August 24-26, 2015, Proceedings 12, Springer. pp. 27–36.

Van Do, T., Nguyen, H.T., Momchil, N., Do, V.T., 2015. Detecting imsi-catcher using soft computing, in: Soft Computing in Data Science: First International Conference, SCDS 2015, Putrajaya, Malaysia, September 2-3, 2015, Proceedings 1, Springer. pp. 129–140.

Yin, C., Zhu, Y., Fei, J., He, X., 2017. A deep learning approach for intrusion detection using recurrent neural networks. IEEE Access 5, 21954–21961.

```
This is pdfTeX, Version 3.141592653-2.6-1.40.25 (TeX Live 2023)
(preloaded format=pdflatex 2024.3.8)  20 SEP 2024 14:06
entering extended mode
 restricted \write18 enabled.
 %&-line parsing enabled.
**main.tex
(./main.tex
LaTeX2e <2023-11-01> patch level 1
L3 programming layer <2024-02-20>
(c:/texlive/2023/texmf-dist/tex/latex/elsarticle/elsarticle.cls
Document Class: elsarticle 2020/11/20, 3.3: Elsevier Ltd
(c:/texlive/2023/texmf-dist/tex/latex/l3kernel/expl3.sty
Package: expl3 2024-02-20 L3 programming layer (loader)
(c:/texlive/2023/texmf-dist/tex/latex/l3backend/l3backend-pdftex.def
File: l3backend-pdftex.def 2024-02-20 L3 backend support: PDF output
(pdfTeX)
\l__color_backend_stack_int=\count188
\l__pdf_internal_box=\box51
)) (c:/texlive/2023/texmf-dist/tex/latex/l3packages/xparse/xparse.sty
Package: xparse 2024-02-18 L3 Experimental document command parser
) (c:/texlive/2023/texmf-dist/tex/latex/etoolbox/etoolbox.sty
Package: etoolbox 2020/10/05 v2.5k e-TeX tools for LaTeX (JAW)
\etb@tempcnta=\count189
)
\@bls=\dimen140
(c:/texlive/2023/texmf-dist/tex/latex/base/article.cls
Document Class: article 2023/05/17 v1.4n Standard LaTeX document class
(c:/texlive/2023/texmf-dist/tex/latex/base/size10.clo
File: size10.clo 2023/05/17 v1.4n Standard LaTeX file (size option)
)
\c@part=\count190
\c@section=\count191
\c@subsection=\count192
\c@subsubsection=\count193
\c@paragraph=\count194
\c@subparagraph=\count195
\c@figure=\count196
\c@table=\count197
\abovecaptionskip=\skip48
\belowcaptionskip=\skip49
\bibindent=\dimen141
) (c:/texlive/2023/texmf-dist/tex/latex/graphics/graphicx.sty
Package: graphicx 2021/09/16 v1.2d Enhanced LaTeX Graphics (DPC,SPQR)
(c:/texlive/2023/texmf-dist/tex/latex/graphics/keyval.sty
Package: keyval 2022/05/29 v1.15 key=value parser (DPC)
\KV@toks@=\toks17
) (c:/texlive/2023/texmf-dist/tex/latex/graphics/graphics.sty
Package: graphics 2022/03/10 v1.4e Standard LaTeX Graphics (DPC,SPQR)
(c:/texlive/2023/texmf-dist/tex/latex/graphics/trig.sty
Package: trig 2021/08/11 v1.11 sin cos tan (DPC)
) (c:/texlive/2023/texmf-dist/tex/latex/graphics-cfg/graphics.cfg
File: graphics.cfg 2016/06/04 v1.11 sample graphics configuration
)
Package graphics Info: Driver file: pdftex.def on input line 107.
```

```
(c:/texlive/2023/texmf-dist/tex/latex/graphics-def/pdftex.def
File: pdftex.def 2022/09/22 v1.2b Graphics/color driver for pdftex
))
\Gin@req@height=\dimen142
\Gin@req@width=\dimen143
)
\c@tnote=\count198
\c@fnote=\count199
\c@cnote=\count266
\c@ead=\count267
\c@author=\count268
\@eadauthor=\toks18
\c@affn=\count269
\absbox=\box52
\elsarticlehighlightsbox=\box53
\elsarticlegrabsbox=\box54
\keybox=\box55
\Columnwidth=\dimen144
\space@left=\dimen145
\els@boxa=\box56
\els@boxb=\box57
\leftMargin=\dimen146
\@enLab=\toks19
\@sep=\skip50
\@@sep=\skip51
(./main.spl) (c:/texlive/2023/texmf-dist/tex/latex/natbib/natbib.sty
Package: natbib 2010/09/13 8.31b (PWD, AO)
\bibhang=\skip52
\bibsep=\skip53
LaTeX Info: Redefining \cite on input line 694.
\c@NAT@ctr=\count270
)
\splwrite=\write3
\openout3 = `main.spl'.

(c:/texlive/2023/texmf-dist/tex/latex/geometry/geometry.sty
Package: geometry 2020/01/02 v5.9 Page Geometry
(c:/texlive/2023/texmf-dist/tex/generic/iftex/ifvtex.sty
Package: ifvtex 2019/10/25 v1.7 ifvtex legacy package. Use iftex instead.
(c:/texlive/2023/texmf-dist/tex/generic/iftex/iftex.sty
Package: iftex 2022/02/03 v1.0f TeX engine tests
))
\Gm@cnth=\count271
\Gm@cntv=\count272
\c@Gm@tempcnt=\count273
\Gm@bindingoffset=\dimen147
\Gm@wd@mp=\dimen148
\Gm@odd@mp=\dimen149
\Gm@even@mp=\dimen150
\Gm@layoutwidth=\dimen151
\Gm@layoutheight=\dimen152
\Gm@layouthoffset=\dimen153
\Gm@layoutvoffset=\dimen154
\Gm@dimlist=\toks20
```

```
) (c:/texlive/2023/texmf-dist/tex/latex/base/fleqn.clo
File: fleqn.clo 2016/12/29 v1.2b Standard LaTeX option (flush left
equations)
\mathindent=\skip54
Applying: [2015/01/01] Make \[ robust on input line 50.
LaTeX Info: Redefining \[ on input line 51.
Already applied: [0000/00/00] Make \[ robust on input line 62.
Applying: [2015/01/01] Make \] robust on input line 74.
LaTeX Info: Redefining \] on input line 75.
Already applied: [0000/00/00] Make \] robust on input line 83.
)
\appnamewidth=\dimen155
) (c:/texlive/2023/texmf-dist/tex/latex/txfonts/txfonts.sty
Package: txfonts 2008/01/22 v3.2.1
LaTeX Font Info:    Redeclaring symbol font `operators' on input line 21.
LaTeX Font Info:    Overwriting symbol font `operators' in version
`normal'
(Font)                  OT1/cmr/m/n --> OT1/txr/m/n on input line 21.
LaTeX Font Info:    Overwriting symbol font `operators' in version `bold'
(Font)                  OT1/cmr/bx/n --> OT1/txr/m/n on input line 21.
LaTeX Font Info:    Overwriting symbol font `operators' in version `bold'
(Font)                  OT1/txr/m/n --> OT1/txr/bx/n on input line 22.
\symitalic=\mathgroup4
LaTeX Font Info:    Overwriting symbol font `italic' in version `bold'
(Font)                  OT1/txr/m/it --> OT1/txr/bx/it on input line 26.
LaTeX Font Info:    Redeclaring math alphabet \mathbf on input line 29.
LaTeX Font Info:    Overwriting math alphabet `\mathbf' in version
`normal'
(Font)                  OT1/cmr/bx/n --> OT1/txr/bx/n on input line 29.
LaTeX Font Info:    Overwriting math alphabet `\mathbf' in version `bold'
(Font)                  OT1/cmr/bx/n --> OT1/txr/bx/n on input line 29.
LaTeX Font Info:    Redeclaring math alphabet \mathit on input line 30.
LaTeX Font Info:    Overwriting math alphabet `\mathit' in version
`normal'
(Font)                  OT1/cmr/m/it --> OT1/txr/m/it on input line 30.
LaTeX Font Info:    Overwriting math alphabet `\mathit' in version `bold'
(Font)                  OT1/cmr/bx/it --> OT1/txr/m/it on input line 30.
LaTeX Font Info:    Overwriting math alphabet `\mathit' in version `bold'
(Font)                  OT1/txr/m/it --> OT1/txr/bx/it on input line 31.
LaTeX Font Info:    Redeclaring math alphabet \mathsf on input line 40.
LaTeX Font Info:    Overwriting math alphabet `\mathsf' in version
`normal'
(Font)                  OT1/cmss/m/n --> OT1/txss/m/n on input line 40.
LaTeX Font Info:    Overwriting math alphabet `\mathsf' in version `bold'
(Font)                  OT1/cmss/bx/n --> OT1/txss/m/n on input line 40.
LaTeX Font Info:    Overwriting math alphabet `\mathsf' in version `bold'
(Font)                  OT1/txss/m/n --> OT1/txss/b/n on input line 41.
LaTeX Font Info:    Redeclaring math alphabet \mathtt on input line 50.
LaTeX Font Info:    Overwriting math alphabet `\mathtt' in version
`normal'
(Font)                  OT1/cmtt/m/n --> OT1/txtt/m/n on input line 50.
LaTeX Font Info:    Overwriting math alphabet `\mathtt' in version `bold'
(Font)                  OT1/cmtt/m/n --> OT1/txtt/m/n on input line 50.
LaTeX Font Info:    Overwriting math alphabet `\mathtt' in version `bold'
```

```
(Font)                  OT1/txtt/m/n --> OT1/txtt/b/n on input line 51.
LaTeX Font Info:    Redeclaring symbol font `letters' on input line 58.
LaTeX Font Info:    Overwriting symbol font `letters' in version `normal'
(Font)                  OML/cmm/m/it --> OML/txmi/m/it on input line 58.
LaTeX Font Info:    Overwriting symbol font `letters' in version `bold'
(Font)                  OML/cmm/b/it --> OML/txmi/m/it on input line 58.
LaTeX Font Info:    Overwriting symbol font `letters' in version `bold'
(Font)                  OML/txmi/m/it --> OML/txmi/bx/it on input line
59.
\symlettersA=\mathgroup5
LaTeX Font Info:    Overwriting symbol font `lettersA' in version `bold'
(Font)                  U/txmia/m/it --> U/txmia/bx/it on input line 67.
LaTeX Font Info:    Redeclaring symbol font `symbols' on input line 77.
LaTeX Font Info:    Overwriting symbol font `symbols' in version `normal'
(Font)                  OMS/cmsy/m/n --> OMS/txsy/m/n on input line 77.
LaTeX Font Info:    Overwriting symbol font `symbols' in version `bold'
(Font)                  OMS/cmsy/b/n --> OMS/txsy/m/n on input line 77.
LaTeX Font Info:    Overwriting symbol font `symbols' in version `bold'
(Font)                  OMS/txsy/m/n --> OMS/txsy/bx/n on input line 78.
\symAMSa=\mathgroup6
LaTeX Font Info:    Overwriting symbol font `AMSa' in version `bold'
(Font)                  U/txsya/m/n --> U/txsya/bx/n on input line 94.
\symAMSb=\mathgroup7
LaTeX Font Info:    Overwriting symbol font `AMSb' in version `bold'
(Font)                  U/txsyb/m/n --> U/txsyb/bx/n on input line 103.
\symsymbolsC=\mathgroup8
LaTeX Font Info:    Overwriting symbol font `symbolsC' in version `bold'
(Font)                  U/txsyc/m/n --> U/txsyc/bx/n on input line 113.
LaTeX Font Info:    Redeclaring symbol font `largesymbols' on input line
120.
LaTeX Font Info:    Overwriting symbol font `largesymbols' in version
`normal'
(Font)                  OMX/cmex/m/n --> OMX/txex/m/n on input line 120.
LaTeX Font Info:    Overwriting symbol font `largesymbols' in version
`bold'
(Font)                  OMX/cmex/m/n --> OMX/txex/m/n on input line 120.
LaTeX Font Info:    Overwriting symbol font `largesymbols' in version
`bold'
(Font)                  OMX/txex/m/n --> OMX/txex/bx/n on input line 121.
\symlargesymbolsA=\mathgroup9
LaTeX Font Info:    Overwriting symbol font `largesymbolsA' in version
`bold'
(Font)                  U/txexa/m/n --> U/txexa/bx/n on input line 129.
LaTeX Font Info:    Redeclaring math symbol \mathsterling on input line
164.
LaTeX Font Info:    Redeclaring math symbol \hbar on input line 591.
LaTeX Info: Redefining \not on input line 1043.
) (c:/texlive/2023/texmf-dist/tex/latex/amsmath/amsmath.sty
Package: amsmath 2023/05/13 v2.17o AMS math features
\@mathmargin=\skip55
For additional information on amsmath, use the `?' option.
(c:/texlive/2023/texmf-dist/tex/latex/amsmath/amstext.sty
Package: amstext 2021/08/26 v2.01 AMS text
(c:/texlive/2023/texmf-dist/tex/latex/amsmath/amsgen.sty
```

```
File: amsgen.sty 1999/11/30 v2.0 generic functions
\@emptytoks=\toks21
\ex@=\dimen156
)) (c:/texlive/2023/texmf-dist/tex/latex/amsmath/amsbsy.sty
Package: amsbsy 1999/11/29 v1.2d Bold Symbols
\pmbraise@=\dimen157
) (c:/texlive/2023/texmf-dist/tex/latex/amsmath/amsopn.sty
Package: amsopn 2022/04/08 v2.04 operator names
)
\inf@bad=\count274
LaTeX Info: Redefining \frac on input line 234.
\uproot@=\count275
\leftroot@=\count276
LaTeX Info: Redefining \overline on input line 399.
LaTeX Info: Redefining \colon on input line 410.
\classnum@=\count277
\DOTSCASE@=\count278
LaTeX Info: Redefining \ldots on input line 496.
LaTeX Info: Redefining \dots on input line 499.
LaTeX Info: Redefining \cdots on input line 620.
\Mathstrutbox@=\box58
\strutbox@=\box59
LaTeX Info: Redefining \big on input line 722.
LaTeX Info: Redefining \Big on input line 723.
LaTeX Info: Redefining \bigg on input line 724.
LaTeX Info: Redefining \Bigg on input line 725.
\big@size=\dimen158
LaTeX Font Info:    Redeclaring font encoding OML on input line 743.
LaTeX Font Info:    Redeclaring font encoding OMS on input line 744.
\macc@depth=\count279
LaTeX Info: Redefining \bmod on input line 905.
LaTeX Info: Redefining \pmod on input line 910.
LaTeX Info: Redefining \smash on input line 940.
LaTeX Info: Redefining \relbar on input line 970.
LaTeX Info: Redefining \Relbar on input line 971.
\c@MaxMatrixCols=\count280
\dotsspace@=\muskip16
\c@parentequation=\count281
\dspbrk@lvl=\count282
\tag@help=\toks22
\row@=\count283
\column@=\count284
\maxfields@=\count285
\andhelp@=\toks23
\eqnshift@=\dimen159
\alignsep@=\dimen160
\tagshift@=\dimen161
\tagwidth@=\dimen162
\totwidth@=\dimen163
\lineht@=\dimen164
\@envbody=\toks24
\multlinegap=\skip56
\multlinetaggap=\skip57
\mathdisplay@stack=\toks25
```

```
LaTeX Info: Redefining \[ on input line 2953.
LaTeX Info: Redefining \] on input line 2954.
) (c:/texlive/2023/texmf-dist/tex/latex/float/float.sty
Package: float 2001/11/08 v1.3d Float enhancements (AL)
\c@float@type=\count286
\float@exts=\toks26
\float@box=\box60
\@float@everytoks=\toks27
\@floatcapt=\box61
) (c:/texlive/2023/texmf-dist/tex/latex/hyperref/hyperref.sty
Package: hyperref 2024-01-20 v7.01h Hypertext links for LaTeX
(c:/texlive/2023/texmf-dist/tex/latex/kvsetkeys/kvsetkeys.sty
Package: kvsetkeys 2022-10-05 v1.19 Key value parser (HO)
) (c:/texlive/2023/texmf-dist/tex/generic/kvdefinekeys/kvdefinekeys.sty
Package: kvdefinekeys 2019-12-19 v1.6 Define keys (HO)
) (c:/texlive/2023/texmf-dist/tex/generic/pdfescape/pdfescape.sty
Package: pdfescape 2019/12/09 v1.15 Implements pdfTeX's escape features
(HO)
(c:/texlive/2023/texmf-dist/tex/generic/ltxcmds/ltxcmds.sty
Package: ltxcmds 2023-12-04 v1.26 LaTeX kernel commands for general use
(HO)
) (c:/texlive/2023/texmf-dist/tex/generic/pdftexcmds/pdftexcmds.sty
Package: pdftexcmds 2020-06-27 v0.33 Utility functions of pdfTeX for
LuaTeX (HO
)
(c:/texlive/2023/texmf-dist/tex/generic/infwarerr/infwarerr.sty
Package: infwarerr 2019/12/03 v1.5 Providing info/warning/error messages
(HO)
)
Package pdftexcmds Info: \pdf@primitive is available.
Package pdftexcmds Info: \pdf@ifprimitive is available.
Package pdftexcmds Info: \pdfdraftmode found.
)) (c:/texlive/2023/texmf-dist/tex/latex/hycolor/hycolor.sty
Package: hycolor 2020-01-27 v1.10 Color options for hyperref/bookmark
(HO)
) (c:/texlive/2023/texmf-dist/tex/latex/auxhook/auxhook.sty
Package: auxhook 2019-12-17 v1.6 Hooks for auxiliary files (HO)
) (c:/texlive/2023/texmf-dist/tex/latex/hyperref/nameref.sty
Package: nameref 2023-11-26 v2.56 Cross-referencing by name of section
(c:/texlive/2023/texmf-dist/tex/latex/refcount/refcount.sty
Package: refcount 2019/12/15 v3.6 Data extraction from label references
(HO)
) (c:/texlive/2023/texmf-
dist/tex/generic/gettitlestring/gettitlestring.sty
Package: gettitlestring 2019/12/15 v1.6 Cleanup title references (HO)
(c:/texlive/2023/texmf-dist/tex/latex/kvoptions/kvoptions.sty
Package: kvoptions 2022-06-15 v3.15 Key value format for package options
(HO)
))
\c@section@level=\count287
)
\@linkdim=\dimen165
\Hy@linkcounter=\count288
\Hy@pagecounter=\count289
```

```
(c:/texlive/2023/texmf-dist/tex/latex/hyperref/pd1enc.def
File: pd1enc.def 2024-01-20 v7.01h Hyperref: PDFDocEncoding definition
(HO)
Now handling font encoding PD1 ...
... no UTF-8 mapping file for font encoding PD1
) (c:/texlive/2023/texmf-dist/tex/generic/intcalc/intcalc.sty
Package: intcalc 2019/12/15 v1.3 Expandable calculations with integers
(HO)
)
\Hy@SavedSpaceFactor=\count290
(c:/texlive/2023/texmf-dist/tex/latex/hyperref/puenc.def
File: puenc.def 2024-01-20 v7.01h Hyperref: PDF Unicode definition (HO)
Now handling font encoding PU ...
... no UTF-8 mapping file for font encoding PU
)
Package hyperref Info: Option `final' set `true' on input line 4062.
Package hyperref Info: Option `pdfusetitle' set `true' on input line
4062.
Package hyperref Info: Hyper figures OFF on input line 4179.
Package hyperref Info: Link nesting OFF on input line 4184.
Package hyperref Info: Hyper index ON on input line 4187.
Package hyperref Info: Plain pages OFF on input line 4194.
Package hyperref Info: Backreferencing OFF on input line 4199.
Package hyperref Info: Implicit mode ON; LaTeX internals redefined.
Package hyperref Info: Bookmarks ON on input line 4446.
\c@Hy@tempcnt=\count291
(c:/texlive/2023/texmf-dist/tex/latex/url/url.sty
\Urlmuskip=\muskip17
Package: url 2013/09/16  ver 3.4  Verb mode for urls, etc.
)
LaTeX Info: Redefining \url on input line 4784.
\XeTeXLinkMargin=\dimen166
(c:/texlive/2023/texmf-dist/tex/generic/bitset/bitset.sty
Package: bitset 2019/12/09 v1.3 Handle bit-vector datatype (HO)
(c:/texlive/2023/texmf-dist/tex/generic/bigintcalc/bigintcalc.sty
Package: bigintcalc 2019/12/15 v1.5 Expandable calculations on big
integers (HO
)
))
\Fld@menulength=\count292
\Field@Width=\dimen167
\Fld@charsize=\dimen168
Package hyperref Info: Hyper figures OFF on input line 6063.
Package hyperref Info: Link nesting OFF on input line 6068.
Package hyperref Info: Hyper index ON on input line 6071.
Package hyperref Info: backreferencing OFF on input line 6078.
Package hyperref Info: Link coloring OFF on input line 6083.
Package hyperref Info: Link coloring with OCG OFF on input line 6088.
Package hyperref Info: PDF/A mode OFF on input line 6093.
! Argument of \x has an extra }.
<inserted text>
                \par
l.6229 ...r\process@me\string\@latex@\@nil{author}
                                                  %
```

```
I've run across a `}' that doesn't seem to match anything.
For example, `\def\a#1{...}' and `\a}' would produce
this error. If you simply proceed now, the `\par' that
I've just inserted will cause me to report a runaway
argument that might be the root of the problem. But if
your `}' was spurious, just type `2' and it will go away.

Runaway argument?
! Paragraph ended before \x was complete.
<to be read again>
                   \par
l.6229 ...r\process@me\string\@latex@\@nil{author}
                                                  %
I suspect you've forgotten a `}', causing me to apply this
control sequence to too much text. How can we recover?
My plan is to forget the whole thing and hope for the best.

(c:/texlive/2023/texmf-dist/tex/latex/base/atbegshi-ltx.sty
Package: atbegshi-ltx 2021/01/10 v1.0c Emulation of the original atbegshi
package with kernel methods
)
\Hy@abspage=\count293
\c@Item=\count294
\c@Hfootnote=\count295
)
Package hyperref Info: Driver (autodetected): hpdftex.
(c:/texlive/2023/texmf-dist/tex/latex/hyperref/hpdftex.def
File: hpdftex.def 2024-01-20 v7.01h Hyperref driver for pdfTeX
(c:/texlive/2023/texmf-dist/tex/latex/base/atveryend-ltx.sty
Package: atveryend-ltx 2020/08/19 v1.0a Emulation of the original
atveryend pac
kage
with kernel methods
)
\Fld@listcount=\count296
\c@bookmark@seq@number=\count297
(c:/texlive/2023/texmf-dist/tex/latex/rerunfilecheck/rerunfilecheck.sty
Package: rerunfilecheck 2022-07-10 v1.10 Rerun checks for auxiliary files
(HO)
(c:/texlive/2023/texmf-dist/tex/generic/uniquecounter/uniquecounter.sty
Package: uniquecounter 2019/12/15 v1.4 Provide unlimited unique counter
(HO)
)
Package uniquecounter Info: New unique counter `rerunfilecheck' on input
line 2
85.
)
\Hy@SectionHShift=\skip58
) (c:/texlive/2023/texmf-dist/tex/latex/amsfonts/amssymb.sty
Package: amssymb 2013/01/14 v3.01 AMS font symbols
(c:/texlive/2023/texmf-dist/tex/latex/amsfonts/amsfonts.sty
Package: amsfonts 2013/01/14 v3.01 Basic AMSFonts support
LaTeX Font Info:    Redeclaring symbol font `AMSa' on input line 59.
LaTeX Font Info:    Overwriting symbol font `AMSa' in version `normal'
```

```
(Font)                U/txsya/m/n --> U/msa/m/n on input line 59.
LaTeX Font Info:    Overwriting symbol font `AMSa' in version `bold'
(Font)                U/txsya/bx/n --> U/msa/m/n on input line 59.
LaTeX Font Info:    Redeclaring symbol font `AMSb' on input line 60.
LaTeX Font Info:    Overwriting symbol font `AMSb' in version `normal'
(Font)                U/txsyb/m/n --> U/msb/m/n on input line 60.
LaTeX Font Info:    Overwriting symbol font `AMSb' in version `bold'
(Font)                U/txsyb/bx/n --> U/msb/m/n on input line 60.
LaTeX Font Info:    Redeclaring math delimiter \ulcorner on input line
74.
LaTeX Font Info:    Redeclaring math delimiter \urcorner on input line
75.
LaTeX Font Info:    Redeclaring math delimiter \llcorner on input line
76.
LaTeX Font Info:    Redeclaring math delimiter \lrcorner on input line
77.
LaTeX Font Info:    Redeclaring math symbol \square on input line 141.
LaTeX Font Info:    Redeclaring math symbol \lozenge on input line 142.
)
LaTeX Font Info:    Redeclaring math symbol \boxdot on input line 44.
LaTeX Font Info:    Redeclaring math symbol \boxplus on input line 45.
LaTeX Font Info:    Redeclaring math symbol \boxtimes on input line 46.
LaTeX Font Info:    Redeclaring math symbol \blacksquare on input line
48.
LaTeX Font Info:    Redeclaring math symbol \centerdot on input line 49.
LaTeX Font Info:    Redeclaring math symbol \blacklozenge on input line
51.
LaTeX Font Info:    Redeclaring math symbol \circlearrowright on input
line 52.

LaTeX Font Info:    Redeclaring math symbol \circlearrowleft on input
line 53.
LaTeX Font Info:    Redeclaring math symbol \leftrightharpoons on input
line 56
.
LaTeX Font Info:    Redeclaring math symbol \boxminus on input line 57.
LaTeX Font Info:    Redeclaring math symbol \Vdash on input line 58.
LaTeX Font Info:    Redeclaring math symbol \Vvdash on input line 59.
LaTeX Font Info:    Redeclaring math symbol \vDash on input line 60.
LaTeX Font Info:    Redeclaring math symbol \twoheadrightarrow on input
line 61
.
LaTeX Font Info:    Redeclaring math symbol \twoheadleftarrow on input
line 62.

LaTeX Font Info:    Redeclaring math symbol \leftleftarrows on input line
63.
LaTeX Font Info:    Redeclaring math symbol \rightrightarrows on input
line 64.

LaTeX Font Info:    Redeclaring math symbol \upuparrows on input line 65.
LaTeX Font Info:    Redeclaring math symbol \downdownarrows on input line
66.
```

```
LaTeX Font Info:    Redeclaring math symbol \upharpoonright on input line
67.
LaTeX Font Info:    Redeclaring math symbol \downharpoonright on input
line 69.

LaTeX Font Info:    Redeclaring math symbol \upharpoonleft on input line
70.
LaTeX Font Info:    Redeclaring math symbol \downharpoonleft on input
line 71.
LaTeX Font Info:    Redeclaring math symbol \rightarrowtail on input line
72.
LaTeX Font Info:    Redeclaring math symbol \leftarrowtail on input line
73.
LaTeX Font Info:    Redeclaring math symbol \leftrightarrows on input
line 74.
LaTeX Font Info:    Redeclaring math symbol \rightleftarrows on input
line 75.
LaTeX Font Info:    Redeclaring math symbol \Lsh on input line 76.
LaTeX Font Info:    Redeclaring math symbol \Rsh on input line 77.
LaTeX Font Info:    Redeclaring math symbol \leftrightsquigarrow on input
line
79.
LaTeX Font Info:    Redeclaring math symbol \looparrowleft on input line
80.
LaTeX Font Info:    Redeclaring math symbol \looparrowright on input line
81.
LaTeX Font Info:    Redeclaring math symbol \circeq on input line 82.
LaTeX Font Info:    Redeclaring math symbol \succsim on input line 83.
LaTeX Font Info:    Redeclaring math symbol \gtrsim on input line 84.
LaTeX Font Info:    Redeclaring math symbol \gtrapprox on input line 85.
LaTeX Font Info:    Redeclaring math symbol \multimap on input line 86.
LaTeX Font Info:    Redeclaring math symbol \therefore on input line 87.
LaTeX Font Info:    Redeclaring math symbol \because on input line 88.
LaTeX Font Info:    Redeclaring math symbol \doteqdot on input line 89.
LaTeX Font Info:    Redeclaring math symbol \triangleq on input line 91.
LaTeX Font Info:    Redeclaring math symbol \precsim on input line 92.
LaTeX Font Info:    Redeclaring math symbol \lesssim on input line 93.
LaTeX Font Info:    Redeclaring math symbol \lessapprox on input line 94.
LaTeX Font Info:    Redeclaring math symbol \eqslantless on input line
95.
LaTeX Font Info:    Redeclaring math symbol \eqslantgtr on input line 96.
LaTeX Font Info:    Redeclaring math symbol \curlyeqprec on input line
97.
LaTeX Font Info:    Redeclaring math symbol \curlyeqsucc on input line
98.
LaTeX Font Info:    Redeclaring math symbol \preccurlyeq on input line
99.
LaTeX Font Info:    Redeclaring math symbol \leqq on input line 100.
LaTeX Font Info:    Redeclaring math symbol \leqslant on input line 101.
LaTeX Font Info:    Redeclaring math symbol \lessgtr on input line 102.
LaTeX Font Info:    Redeclaring math symbol \backprime on input line 103.
LaTeX Font Info:    Redeclaring math symbol \risingdotseq on input line
104.
```

```
LaTeX Font Info:    Redeclaring math symbol \fallingdotseq on input line
105.
LaTeX Font Info:    Redeclaring math symbol \succcurlyeq on input line
106.
LaTeX Font Info:    Redeclaring math symbol \geqq on input line 107.
LaTeX Font Info:    Redeclaring math symbol \geqslant on input line 108.
LaTeX Font Info:    Redeclaring math symbol \gtrless on input line 109.
LaTeX Font Info:    Redeclaring math symbol \bigstar on input line 117.
LaTeX Font Info:    Redeclaring math symbol \between on input line 118.
LaTeX Font Info:    Redeclaring math symbol \blacktriangledown on input
line 11
9.
LaTeX Font Info:    Redeclaring math symbol \blacktriangleright on input
line 1
20.
LaTeX Font Info:    Redeclaring math symbol \blacktriangleleft on input
line 12
1.
LaTeX Font Info:    Redeclaring math symbol \vartriangle on input line
122.
LaTeX Font Info:    Redeclaring math symbol \blacktriangle on input line
123.
LaTeX Font Info:    Redeclaring math symbol \triangledown on input line
124.
LaTeX Font Info:    Redeclaring math symbol \eqcirc on input line 125.
LaTeX Font Info:    Redeclaring math symbol \lesseqgtr on input line 126.
LaTeX Font Info:    Redeclaring math symbol \gtreqless on input line 127.
LaTeX Font Info:    Redeclaring math symbol \lesseqqgtr on input line
128.
LaTeX Font Info:    Redeclaring math symbol \gtreqqless on input line
129.
LaTeX Font Info:    Redeclaring math symbol \Rrightarrow on input line
130.
LaTeX Font Info:    Redeclaring math symbol \Lleftarrow on input line
131.
LaTeX Font Info:    Redeclaring math symbol \veebar on input line 132.
LaTeX Font Info:    Redeclaring math symbol \barwedge on input line 133.
LaTeX Font Info:    Redeclaring math symbol \doublebarwedge on input line
134.
LaTeX Font Info:    Redeclaring math symbol \measuredangle on input line
137.
LaTeX Font Info:    Redeclaring math symbol \sphericalangle on input line
138.
LaTeX Font Info:    Redeclaring math symbol \varpropto on input line 139.
LaTeX Font Info:    Redeclaring math symbol \smallsmile on input line
140.
LaTeX Font Info:    Redeclaring math symbol \smallfrown on input line
141.
LaTeX Font Info:    Redeclaring math symbol \Subset on input line 142.
LaTeX Font Info:    Redeclaring math symbol \Supset on input line 143.
LaTeX Font Info:    Redeclaring math symbol \Cup on input line 144.
LaTeX Font Info:    Redeclaring math symbol \Cap on input line 146.
LaTeX Font Info:    Redeclaring math symbol \curlywedge on input line
148.
```

```
LaTeX Font Info:    Redeclaring math symbol \curlyvee on input line 149.
LaTeX Font Info:    Redeclaring math symbol \leftthreetimes on input line
150.
LaTeX Font Info:    Redeclaring math symbol \rightthreetimes on input
line 151.

LaTeX Font Info:    Redeclaring math symbol \subseteqq on input line 152.
LaTeX Font Info:    Redeclaring math symbol \supseteqq on input line 153.
LaTeX Font Info:    Redeclaring math symbol \bumpeq on input line 154.
LaTeX Font Info:    Redeclaring math symbol \Bumpeq on input line 155.
LaTeX Font Info:    Redeclaring math symbol \lll on input line 156.
LaTeX Font Info:    Redeclaring math symbol \ggg on input line 158.
LaTeX Font Info:    Redeclaring math symbol \circledS on input line 160.
LaTeX Font Info:    Redeclaring math symbol \pitchfork on input line 161.
LaTeX Font Info:    Redeclaring math symbol \dotplus on input line 162.
LaTeX Font Info:    Redeclaring math symbol \backsim on input line 163.
LaTeX Font Info:    Redeclaring math symbol \backsimeq on input line 164.
LaTeX Font Info:    Redeclaring math symbol \complement on input line
165.
LaTeX Font Info:    Redeclaring math symbol \intercal on input line 166.
LaTeX Font Info:    Redeclaring math symbol \circledcirc on input line
167.
LaTeX Font Info:    Redeclaring math symbol \circledast on input line
168.
LaTeX Font Info:    Redeclaring math symbol \circleddash on input line
169.
LaTeX Font Info:    Redeclaring math symbol \lvertneqq on input line 171.
LaTeX Font Info:    Redeclaring math symbol \gvertneqq on input line 172.
LaTeX Font Info:    Redeclaring math symbol \nleq on input line 173.
LaTeX Font Info:    Redeclaring math symbol \ngeq on input line 174.
LaTeX Font Info:    Redeclaring math symbol \nless on input line 175.
LaTeX Font Info:    Redeclaring math symbol \ngtr on input line 176.
LaTeX Font Info:    Redeclaring math symbol \nprec on input line 177.
LaTeX Font Info:    Redeclaring math symbol \nsucc on input line 178.
LaTeX Font Info:    Redeclaring math symbol \lneqq on input line 179.
LaTeX Font Info:    Redeclaring math symbol \gneqq on input line 180.
LaTeX Font Info:    Redeclaring math symbol \nleqslant on input line 181.
LaTeX Font Info:    Redeclaring math symbol \ngeqslant on input line 182.
LaTeX Font Info:    Redeclaring math symbol \lneq on input line 183.
LaTeX Font Info:    Redeclaring math symbol \gneq on input line 184.
LaTeX Font Info:    Redeclaring math symbol \npreceq on input line 185.
LaTeX Font Info:    Redeclaring math symbol \nsucceq on input line 186.
LaTeX Font Info:    Redeclaring math symbol \precnsim on input line 187.
LaTeX Font Info:    Redeclaring math symbol \succnsim on input line 188.
LaTeX Font Info:    Redeclaring math symbol \lnsim on input line 189.
LaTeX Font Info:    Redeclaring math symbol \gnsim on input line 190.
LaTeX Font Info:    Redeclaring math symbol \nleqq on input line 191.
LaTeX Font Info:    Redeclaring math symbol \ngeqq on input line 192.
LaTeX Font Info:    Redeclaring math symbol \precneqq on input line 193.
LaTeX Font Info:    Redeclaring math symbol \succneqq on input line 194.
LaTeX Font Info:    Redeclaring math symbol \precnapprox on input line
195.
LaTeX Font Info:    Redeclaring math symbol \succnapprox on input line
196.
```

```
LaTeX Font Info:    Redeclaring math symbol \lnapprox on input line 197.
LaTeX Font Info:    Redeclaring math symbol \gnapprox on input line 198.
LaTeX Font Info:    Redeclaring math symbol \nsim on input line 199.
LaTeX Font Info:    Redeclaring math symbol \ncong on input line 200.
LaTeX Font Info:    Redeclaring math symbol \diagup on input line 201.
LaTeX Font Info:    Redeclaring math symbol \diagdown on input line 202.
LaTeX Font Info:    Redeclaring math symbol \varsubsetneq on input line
203.
LaTeX Font Info:    Redeclaring math symbol \varsupsetneq on input line
204.
LaTeX Font Info:    Redeclaring math symbol \nsubseteqq on input line
205.
LaTeX Font Info:    Redeclaring math symbol \nsupseteqq on input line
206.
LaTeX Font Info:    Redeclaring math symbol \subsetneqq on input line
207.
LaTeX Font Info:    Redeclaring math symbol \supsetneqq on input line
208.
LaTeX Font Info:    Redeclaring math symbol \varsubsetneqq on input line
209.
LaTeX Font Info:    Redeclaring math symbol \varsupsetneqq on input line
210.
LaTeX Font Info:    Redeclaring math symbol \subsetneq on input line 211.
LaTeX Font Info:    Redeclaring math symbol \supsetneq on input line 212.
LaTeX Font Info:    Redeclaring math symbol \nsubseteq on input line 213.
LaTeX Font Info:    Redeclaring math symbol \nsupseteq on input line 214.
LaTeX Font Info:    Redeclaring math symbol \nparallel on input line 215.
LaTeX Font Info:    Redeclaring math symbol \nmid on input line 216.
LaTeX Font Info:    Redeclaring math symbol \nshortmid on input line 217.
LaTeX Font Info:    Redeclaring math symbol \nshortparallel on input line
218.
LaTeX Font Info:    Redeclaring math symbol \nvdash on input line 219.
LaTeX Font Info:    Redeclaring math symbol \nVdash on input line 220.
LaTeX Font Info:    Redeclaring math symbol \nvDash on input line 221.
LaTeX Font Info:    Redeclaring math symbol \nVDash on input line 222.
LaTeX Font Info:    Redeclaring math symbol \ntrianglerighteq on input
line 223
.
LaTeX Font Info:    Redeclaring math symbol \ntrianglelefteq on input
line 224.

LaTeX Font Info:    Redeclaring math symbol \ntriangleleft on input line
225.
LaTeX Font Info:    Redeclaring math symbol \ntriangleright on input line
226.
LaTeX Font Info:    Redeclaring math symbol \nleftarrow on input line
227.
LaTeX Font Info:    Redeclaring math symbol \nrightarrow on input line
228.
LaTeX Font Info:    Redeclaring math symbol \nLeftarrow on input line
229.
LaTeX Font Info:    Redeclaring math symbol \nRightarrow on input line
230.
```

```
LaTeX Font Info:    Redeclaring math symbol \nLeftrightarrow on input
line 231.

LaTeX Font Info:    Redeclaring math symbol \nleftrightarrow on input
line 232.

LaTeX Font Info:    Redeclaring math symbol \divideontimes on input line
233.
LaTeX Font Info:    Redeclaring math symbol \varnothing on input line
234.
LaTeX Font Info:    Redeclaring math symbol \nexists on input line 235.
LaTeX Font Info:    Redeclaring math symbol \Finv on input line 236.
LaTeX Font Info:    Redeclaring math symbol \Game on input line 237.
LaTeX Font Info:    Redeclaring math symbol \eth on input line 240.
LaTeX Font Info:    Redeclaring math symbol \eqsim on input line 241.
LaTeX Font Info:    Redeclaring math symbol \beth on input line 242.
LaTeX Font Info:    Redeclaring math symbol \gimel on input line 243.
LaTeX Font Info:    Redeclaring math symbol \daleth on input line 244.
LaTeX Font Info:    Redeclaring math symbol \lessdot on input line 245.
LaTeX Font Info:    Redeclaring math symbol \gtrdot on input line 246.
LaTeX Font Info:    Redeclaring math symbol \ltimes on input line 247.
LaTeX Font Info:    Redeclaring math symbol \rtimes on input line 248.
LaTeX Font Info:    Redeclaring math symbol \shortmid on input line 249.
LaTeX Font Info:    Redeclaring math symbol \shortparallel on input line
250.
LaTeX Font Info:    Redeclaring math symbol \smallsetminus on input line
251.
LaTeX Font Info:    Redeclaring math symbol \thicksim on input line 252.
LaTeX Font Info:    Redeclaring math symbol \thickapprox on input line
253.
LaTeX Font Info:    Redeclaring math symbol \approxeq on input line 254.
LaTeX Font Info:    Redeclaring math symbol \succapprox on input line
255.
LaTeX Font Info:    Redeclaring math symbol \precapprox on input line
256.
LaTeX Font Info:    Redeclaring math symbol \curvearrowleft on input line
257.
LaTeX Font Info:    Redeclaring math symbol \curvearrowright on input
line 258.

LaTeX Font Info:    Redeclaring math symbol \digamma on input line 259.
LaTeX Font Info:    Redeclaring math symbol \varkappa on input line 260.
LaTeX Font Info:    Redeclaring math symbol \Bbbk on input line 261.
LaTeX Font Info:    Redeclaring math symbol \hslash on input line 262.
LaTeX Font Info:    Redeclaring math symbol \backepsilon on input line
265.
)
LaTeX Font Info:    Trying to load font information for OT1+txr on input
line 7
4.
(c:/texlive/2023/texmf-dist/tex/latex/txfonts/ot1txr.fd
File: ot1txr.fd 2000/12/15 v3.1
) (./main.aux)
\openout1 = `main.aux'.
```

```
LaTeX Font Info:    Checking defaults for OML/txmi/m/it on input line 74.
LaTeX Font Info:    Trying to load font information for OML+txmi on input
line
74.
(c:/texlive/2023/texmf-dist/tex/latex/txfonts/omltxmi.fd
File: omltxmi.fd 2000/12/15 v3.1
)
LaTeX Font Info:    ... okay on input line 74.
LaTeX Font Info:    Checking defaults for OMS/txsy/m/n on input line 74.
LaTeX Font Info:    Trying to load font information for OMS+txsy on input
line
74.
(c:/texlive/2023/texmf-dist/tex/latex/txfonts/omstxsy.fd
File: omstxsy.fd 2000/12/15 v3.1
)
LaTeX Font Info:    ... okay on input line 74.
LaTeX Font Info:    Checking defaults for OT1/cmr/m/n on input line 74.
LaTeX Font Info:    ... okay on input line 74.
LaTeX Font Info:    Checking defaults for T1/cmr/m/n on input line 74.
LaTeX Font Info:    ... okay on input line 74.
LaTeX Font Info:    Checking defaults for TS1/cmr/m/n on input line 74.
LaTeX Font Info:    ... okay on input line 74.
LaTeX Font Info:    Checking defaults for OMX/txex/m/n on input line 74.
LaTeX Font Info:    Trying to load font information for OMX+txex on input
line
74.
(c:/texlive/2023/texmf-dist/tex/latex/txfonts/omxtxex.fd
File: omxtxex.fd 2000/12/15 v3.1
)
LaTeX Font Info:    ... okay on input line 74.
LaTeX Font Info:    Checking defaults for U/txexa/m/n on input line 74.
LaTeX Font Info:    Trying to load font information for U+txexa on input
line 7
4.
(c:/texlive/2023/texmf-dist/tex/latex/txfonts/utxexa.fd
File: utxexa.fd 2000/12/15 v3.1
)
LaTeX Font Info:    ... okay on input line 74.
LaTeX Font Info:    Checking defaults for PD1/pdf/m/n on input line 74.
LaTeX Font Info:    ... okay on input line 74.
LaTeX Font Info:    Checking defaults for PU/pdf/m/n on input line 74.
LaTeX Font Info:    ... okay on input line 74.
(c:/texlive/2023/texmf-dist/tex/context/base/mkii/supp-pdf.mkii
[Loading MPS to PDF converter (version 2006.09.02).]
\scratchcounter=\count298
\scratchdimen=\dimen169
\scratchbox=\box62
\nofMPsegments=\count299
\nofMParguments=\count300
\everyMPshowfont=\toks28
\MPscratchCnt=\count301
\MPscratchDim=\dimen170
\MPnumerator=\count302
```

```
\makeMPintoPDFobject=\count303
\everyMPtoPDFconversion=\toks29
) (c:/texlive/2023/texmf-dist/tex/latex/epstopdf-pkg/epstopdf-base.sty
Package: epstopdf-base 2020-01-24 v2.11 Base part for package epstopdf
Package epstopdf-base Info: Redefining graphics rule for `.eps' on input
line 4
85.
(c:/texlive/2023/texmf-dist/tex/latex/latexconfig/epstopdf-sys.cfg
File: epstopdf-sys.cfg 2010/07/13 v1.3 Configuration of (r)epstopdf for
TeX Liv
e
))
*geometry* driver: auto-detecting
*geometry* detected driver: pdftex
*geometry* verbose mode - [ preamble ] result:
* driver: pdftex
* paper: custom
* layout: <same size as paper>
* layoutoffset:(h,v)=(0.0pt,0.0pt)
* hratio: 1:1
* vratio: 1:1
* modes:
* h-part:(L,W,R)=(37.75394pt, 522.0pt, 37.75394pt)
* v-part:(T,H,B)=(81.52342pt, 682.0pt, 81.52342pt)
* \paperwidth=597.50787pt
* \paperheight=845.04684pt
* \textwidth=522.0pt
* \textheight=682.0pt
* \oddsidemargin=-34.51605pt
* \evensidemargin=-34.51605pt
* \topmargin=-52.74657pt
* \headheight=50.0pt
* \headsep=12.0pt
* \topskip=10.0pt
* \footskip=18.0pt
* \marginparwidth=4.0pt
* \marginparsep=10.0pt
* \columnsep=18.0pt
* \skip\footins=24.0pt plus 2.0pt minus 12.0pt
* \hoffset=0.0pt
* \voffset=0.0pt
* \mag=1000
* \@twocolumntrue
* \@twosidefalse
* \@mparswitchfalse
* \@reversemarginfalse
* (1in=72.27pt=25.4mm, 1cm=28.453pt)

Package hyperref Info: Link coloring OFF on input line 74.
(./main.out) (./main.out)
\@outlinefile=\write4
\openout4 = `main.out'.

LaTeX Font Info:    Font shape `OT1/txr/b/n' in size <10> not available
```

```
(Font)              Font shape `OT1/txr/bx/n' tried instead on input line
148.
LaTeX Font Info:    Trying to load font information for U+txmia on input
line 1
65.
(c:/texlive/2023/texmf-dist/tex/latex/txfonts/utxmia.fd
File: utxmia.fd 2000/12/15 v3.1
)
LaTeX Font Info:    Trying to load font information for U+msa on input
line 165
.
(c:/texlive/2023/texmf-dist/tex/latex/amsfonts/umsa.fd
File: umsa.fd 2013/01/14 v3.01 AMS symbols A
)
LaTeX Font Info:    Trying to load font information for U+msb on input
line 165
.
(c:/texlive/2023/texmf-dist/tex/latex/amsfonts/umsb.fd
File: umsb.fd 2013/01/14 v3.01 AMS symbols B
)
LaTeX Font Info:    Trying to load font information for U+txsyc on input
line 1
65.
(c:/texlive/2023/texmf-dist/tex/latex/txfonts/utxsyc.fd
File: utxsyc.fd 2000/12/15 v3.1
)

Package natbib Warning: Citation `li20215growth' on page 1 undefined on
input l
ine 172.


Package natbib Warning: Citation `nakarmi2021murat' on page 1 undefined
on inpu
t line 174.


Package natbib Warning: Citation `Alrashede2019' on page 1 undefined on
input l
ine 175.


Package natbib Warning: Citation `3gpp2023' on page 1 undefined on input
line 1
75.


Package natbib Warning: Citation `AIMSICD' on page 1 undefined on input
line 17
7.


Package natbib Warning: Citation `SnoopSnitch' on page 1 undefined on
input lin
```

```
e 177.


Package natbib Warning: Citation `Li2017' on page 1 undefined on input
line 177
.


Package natbib Warning: Citation `steig2016network' on page 1 undefined
on inpu
t line 177.


Underfull \vbox (badness 10000) has occurred while \output is active []


Overfull \hbox (1.90001pt too wide) has occurred while \output is active
[]
 []

[1{c:/texlive/2023/texmf-
var/fonts/map/pdftex/updmap/pdftex.map}{c:/texlive/202
3/texmf-dist/fonts/enc/dvips/base/8r.enc}


]

Package natbib Warning: Citation `10073944' on page 2 undefined on input
line 1
79.


Package natbib Warning: Citation `dey2023efficient' on page 2 undefined
on inpu
t line 179.


Package natbib Warning: Citation `saedi2022synthetic' on page 2 undefined
on in
put line 179.

LaTeX Font Info:    Trying to load font information for TS1+txr on input
line 1
84.
(c:/texlive/2023/texmf-dist/tex/latex/txfonts/ts1txr.fd
File: ts1txr.fd 2000/12/15 v3.1
)
Underfull \hbox (badness 1048) in paragraph at lines 184--185
[]\OT1/txr/m/n/10 Providing a 3GPP Re-lease 18 com-pli-ant RBS de-tec-
 []


Package natbib Warning: Citation `AIMSICD' on page 2 undefined on input
line 20
```

9.

Package natbib Warning: Citation `Skibapps' on page 2 undefined on input line 2
09.

Package natbib Warning: Citation `CatcherCatcher' on page 2 undefined on input
line 209.

Package natbib Warning: Citation `SnoopSnitch' on page 2 undefined on input lin
e 209.

Package natbib Warning: Citation `brenninkmeijer2016catching' on page 2 undefin
ed on input line 209.

Package natbib Warning: Citation `Li2017' on page 2 undefined on input line 211
.

Package natbib Warning: Citation `van2015detecting' on page 2 undefined on inpu
t line 211.

Package natbib Warning: Citation `do2016strengthening' on page 2 undefined on i
nput line 211.

Package natbib Warning: Citation `Aftenposten2015' on page 2 undefined on input
 line 211.

Package natbib Warning: Citation `steig2016network' on page 2 undefined on inpu
t line 213.

Package natbib Warning: Citation `steig2016network' on page 2 undefined on inpu
t line 213.

Package natbib Warning: Citation `nakarmi2021murat' on page 2 undefined
on inpu
t line 213.

[2]

Package natbib Warning: Citation `dong2016detection' on page 3 undefined
on inp
ut line 215.

Package natbib Warning: Citation `yin2017deep' on page 3 undefined on
input lin
e 215.

Package natbib Warning: Citation
`mubasshir2024fbsdetectorfakebasestation' on p
age 3 undefined on input line 216.

Package natbib Warning: Citation `nakarmi2021murat' on page 3 undefined
on inpu
t line 223.

Package natbib Warning: Citation `Nakarmi2018' on page 3 undefined on
input lin
e 223.

Package natbib Warning: Citation `3GPPTS33.5012022' on page 3 undefined
on inpu
t line 223.

Package natbib Warning: Citation `3GPPTR38.3002021' on page 3 undefined
on inpu
t line 227.

Package natbib Warning: Citation `gorrepati2021privacy' on page 3
undefined on
input line 227.

Package natbib Warning: Citation `ComponentD.H.S.andCallahan2019' on page
3 und
efined on input line 227.

LaTeX Warning: File `Figures/Fig-1-RBS_Detector.png' not found on input
line 23
1.

```
! Package pdftex.def Error: File `Figures/Fig-1-RBS_Detector.png' not
found: us
ing draft setting.

See the pdftex.def package documentation for explanation.
Type  H <return>  for immediate help.
 ...

l.231 ...ight=4cm]{Figures/Fig-1-RBS_Detector.png}

Try typing  <return>  to proceed.
If that doesn't work, type  X <return>  to quit.


Overfull \hbox (9.07114pt too wide) in paragraph at lines 231--232
 [][]
 []


Underfull \vbox (badness 10000) has occurred while \output is active []


Package natbib Warning: Citation `Nakarmi2018' on page 3 undefined on
input lin
e 236.


Package natbib Warning: Citation `shaik2018impact' on page 3 undefined on
input
 line 243.


LaTeX Warning: File `Figures/Fig-2-30LBS.png' not found on input line
246.


! Package pdftex.def Error: File `Figures/Fig-2-30LBS.png' not found:
using dra
ft setting.

See the pdftex.def package documentation for explanation.
Type  H <return>  for immediate help.
 ...

l.246 ...th,height=5.6cm]{Figures/Fig-2-30LBS.png}

Try typing  <return>  to proceed.
If that doesn't work, type  X <return>  to quit.


Overfull \hbox (29.95396pt too wide) in paragraph at lines 246--247
 [][]
```

```
 []

[3]

LaTeX Warning: File `Figures/Fig-3-Handover30LBS.png' not found on input
line 2
53.


! Package pdftex.def Error: File `Figures/Fig-3-Handover30LBS.png' not
found: u
sing draft setting.

See the pdftex.def package documentation for explanation.
Type  H <return>  for immediate help.
 ...

l.253 ...t=5.6cm]{Figures/Fig-3-Handover30LBS.png}

Try typing  <return>  to proceed.
If that doesn't work, type  X <return>  to quit.


Overfull \hbox (29.95396pt too wide) in paragraph at lines 253--254
 [][]
 []


Package natbib Warning: Citation `saedi2022synthetic' on page 4 undefined
on in
put line 258.


LaTeX Warning: File `Figures/Fig-4-ProbationPeriod.png' not found on
input line
 263.


! Package pdftex.def Error: File `Figures/Fig-4-ProbationPeriod.png' not
found:
 using draft setting.

See the pdftex.def package documentation for explanation.
Type  H <return>  for immediate help.
 ...

l.263 ...4.5cm]{Figures/Fig-4-ProbationPeriod.png}

Try typing  <return>  to proceed.
If that doesn't work, type  X <return>  to quit.


LaTeX Warning: File `Figures/Fig-5-BS&RBS.png' not found on input line
273.
```

```
! Package pdftex.def Error: File `Figures/Fig-5-BS&RBS.png' not found:
using dr
aft setting.

See the pdftex.def package documentation for explanation.
Type  H <return>  for immediate help.
 ...

l.273 ...h,height=5.5cm]{Figures/Fig-5-BS&RBS.png}

Try typing  <return>  to proceed.
If that doesn't work, type  X <return>  to quit.


Overfull \hbox (9.07114pt too wide) in paragraph at lines 273--274
 [][]
 []

[4]

LaTeX Warning: File `Figures/Fig-6-30BS&RBS.png' not found on input line
286.


! Package pdftex.def Error: File `Figures/Fig-6-30BS&RBS.png' not found:
using
draft setting.

See the pdftex.def package documentation for explanation.
Type  H <return>  for immediate help.
 ...

l.286 ...height=5.6cm]{Figures/Fig-6-30BS&RBS.png}

Try typing  <return>  to proceed.
If that doesn't work, type  X <return>  to quit.


Overfull \hbox (29.95396pt too wide) in paragraph at lines 286--287
 [][]
 []


LaTeX Warning: File `Figures/Fig-7-HO-RBS.png' not found on input line
295.


! Package pdftex.def Error: File `Figures/Fig-7-HO-RBS.png' not found:
using dr
aft setting.

See the pdftex.def package documentation for explanation.
```

```
Type  H <return>  for immediate help.
 ...

l.295 ...h,height=5.6cm]{Figures/Fig-7-HO-RBS.png}

Try typing  <return>  to proceed.
If that doesn't work, type  X <return>  to quit.


Overfull \hbox (29.95396pt too wide) in paragraph at lines 295--296
 [][]
 []


LaTeX Warning: File `Figures/Fig-8-statemachine.png' not found on input
line 30
9.


! Package pdftex.def Error: File `Figures/Fig-8-statemachine.png' not
found: us
ing draft setting.

See the pdftex.def package documentation for explanation.
Type  H <return>  for immediate help.
 ...

l.309 ...ight=7cm]{Figures/Fig-8-statemachine.png}

Try typing  <return>  to proceed.
If that doesn't work, type  X <return>  to quit.


Package natbib Warning: Citation `Specification2021' on page 5 undefined
on inp
ut line 320.

[5]

Package natbib Warning: Citation `9162275' on page 6 undefined on input
line 32
2.


Package natbib Warning: Citation `van2015strong' on page 6 undefined on
input l
ine 322.


Package natbib Warning: Citation `Barco2001' on page 6 undefined on input
line
322.
```

```
LaTeX Warning: File `Figures/Fig-9-6cars.jpg' not found on input line
326.


! Package pdftex.def Error: File `Figures/Fig-9-6cars.jpg' not found:
using dra
ft setting.

See the pdftex.def package documentation for explanation.
Type  H <return>  for immediate help.
 ...

l.326 ...h=0.3\textwidth]{Figures/Fig-9-6cars.jpg}

Try typing  <return>  to proceed.
If that doesn't work, type  X <return>  to quit.


Overfull \hbox (13.63019pt too wide) in paragraph at lines 335--359
 [][]
 []


Package natbib Warning: Citation `saedi2022synthetic' on page 6 undefined
on in
put line 367.


LaTeX Warning: File `Figures/Fig-10-MLP.png' not found on input line 405.


! Package pdftex.def Error: File `Figures/Fig-10-MLP.png' not found:
using draf
t setting.

See the pdftex.def package documentation for explanation.
Type  H <return>  for immediate help.
 ...

l.405  {Figures/Fig-10-MLP.png}

Try typing  <return>  to proceed.
If that doesn't work, type  X <return>  to quit.

[6]

Package natbib Warning: Citation `selis2018classification' on page 7
undefined
on input line 424.


Package natbib Warning: Citation `gyawali2020machine' on page 7 undefined
on in
put line 424.
```

```
[7]

LaTeX Warning: File `Figures/Fig-11-Accuracy-2.png' not found on input
line 437
.


! Package pdftex.def Error: File `Figures/Fig-11-Accuracy-2.png' not
found: usi
ng draft setting.

See the pdftex.def package documentation for explanation.
Type  H <return>  for immediate help.
 ...

l.437 ...ght=5.5cm]{Figures/Fig-11-Accuracy-2.png}

Try typing  <return>  to proceed.
If that doesn't work, type  X <return>  to quit.


Overfull \hbox (9.07114pt too wide) in paragraph at lines 437--438
 [][]
 []


LaTeX Warning: File `Figures/Fig-12-Precision.png' not found on input
line 447.



! Package pdftex.def Error: File `Figures/Fig-12-Precision.png' not
found: usin
g draft setting.

See the pdftex.def package documentation for explanation.
Type  H <return>  for immediate help.
 ...

l.447 ...height=5cm]{Figures/Fig-12-Precision.png}

Try typing  <return>  to proceed.
If that doesn't work, type  X <return>  to quit.


Overfull \hbox (9.07114pt too wide) in paragraph at lines 447--448
 [][]
 []


LaTeX Warning: File `Figures/Fig-13-F1Score.png' not found on input line
457.
```

```
! Package pdftex.def Error: File `Figures/Fig-13-F1Score.png' not found:
using
draft setting.

See the pdftex.def package documentation for explanation.
Type  H <return>  for immediate help.
 ...

l.457 ....5\textwidth]{Figures/Fig-13-F1Score.png}

Try typing  <return>  to proceed.
If that doesn't work, type  X <return>  to quit.


Overfull \hbox (9.0pt too wide) in paragraph at lines 457--458
 [][]
 []


LaTeX Warning: File `Figures/Fig-14-Recall.png' not found on input line
464.


! Package pdftex.def Error: File `Figures/Fig-14-Recall.png' not found:
using d
raft setting.

See the pdftex.def package documentation for explanation.
Type  H <return>  for immediate help.
 ...

l.464 ...0.5\textwidth]{Figures/Fig-14-Recall.png}

Try typing  <return>  to proceed.
If that doesn't work, type  X <return>  to quit.


Overfull \hbox (9.0pt too wide) in paragraph at lines 464--465
 [][]
 []

[8]

Package natbib Warning: Citation `ian2017deep' on page 9 undefined on
input lin
e 503.


Package natbib Warning: Citation `reed1999neural' on page 9 undefined on
input
line 503.
```

```
LaTeX Warning: File `Figures/Fig-15-Loss.png' not found on input line
507.


! Package pdftex.def Error: File `Figures/Fig-15-Loss.png' not found:
using dra
ft setting.

See the pdftex.def package documentation for explanation.
Type  H <return>  for immediate help.
 ...

l.507 ...dth, height=5cm]{Figures/Fig-15-Loss.png}

Try typing  <return>  to proceed.
If that doesn't work, type  X <return>  to quit.


Overfull \hbox (9.07114pt too wide) in paragraph at lines 507--508
 [][]
 []


Underfull \vbox (badness 10000) has occurred while \output is active []


Package natbib Warning: Citation
`mubasshir2024fbsdetectorfakebasestation' on p
age 9 undefined on input line 516.


Package natbib Warning: Citation `huang2023developing' on page 9
undefined on i
nput line 516.

No file main.bbl.

Package natbib Warning: There were undefined citations.

[9] [10] (./main.aux)
 ***********
LaTeX2e <2023-11-01> patch level 1
L3 programming layer <2024-02-20>
 ***********
Package rerunfilecheck Info: File `main.out' has not changed.
(rerunfilecheck)             Checksum:
29C307833958026D0B0FE1D3E3DFDADD;2638.
 )
Here is how much of TeX's memory you used:
 12239 strings out of 474121
 191287 string characters out of 5747949
 1951190 words of memory out of 5000000
 34372 multiletter control sequences out of 15000+600000
 589270 words of font info for 111 fonts, out of 8000000 for 9000
```

```
 1141 hyphenation exceptions out of 8191
 75i,9n,79p,1463b,472s stack positions out of
10000i,1000n,20000p,200000b,200000s
<c:/texlive/2023/texmf-
dist/fonts/type1/public/amsfonts/cm/cmtt10.pfb><c:/tex
live/2023/texmf-
dist/fonts/type1/public/amsfonts/cm/cmtt8.pfb><c:/texlive/2023/
texmf-dist/fonts/type1/public/txfonts/rtcxr.pfb><c:/texlive/2023/texmf-
dist/fon
ts/type1/public/txfonts/rtxr.pfb><c:/texlive/2023/texmf-
dist/fonts/type1/urw/ti
mes/utmb8a.pfb><c:/texlive/2023/texmf-
dist/fonts/type1/urw/times/utmr8a.pfb><c:
/texlive/2023/texmf-dist/fonts/type1/urw/times/utmri8a.pfb>
Output written on main.pdf (10 pages, 121781 bytes).
PDF statistics:
 200 PDF objects out of 1000 (max. 8388607)
 172 compressed objects within 2 object streams
 46 named destinations out of 1000 (max. 500000)
 105 words of extra memory for PDF output out of 10000 (max. 10000000)
```

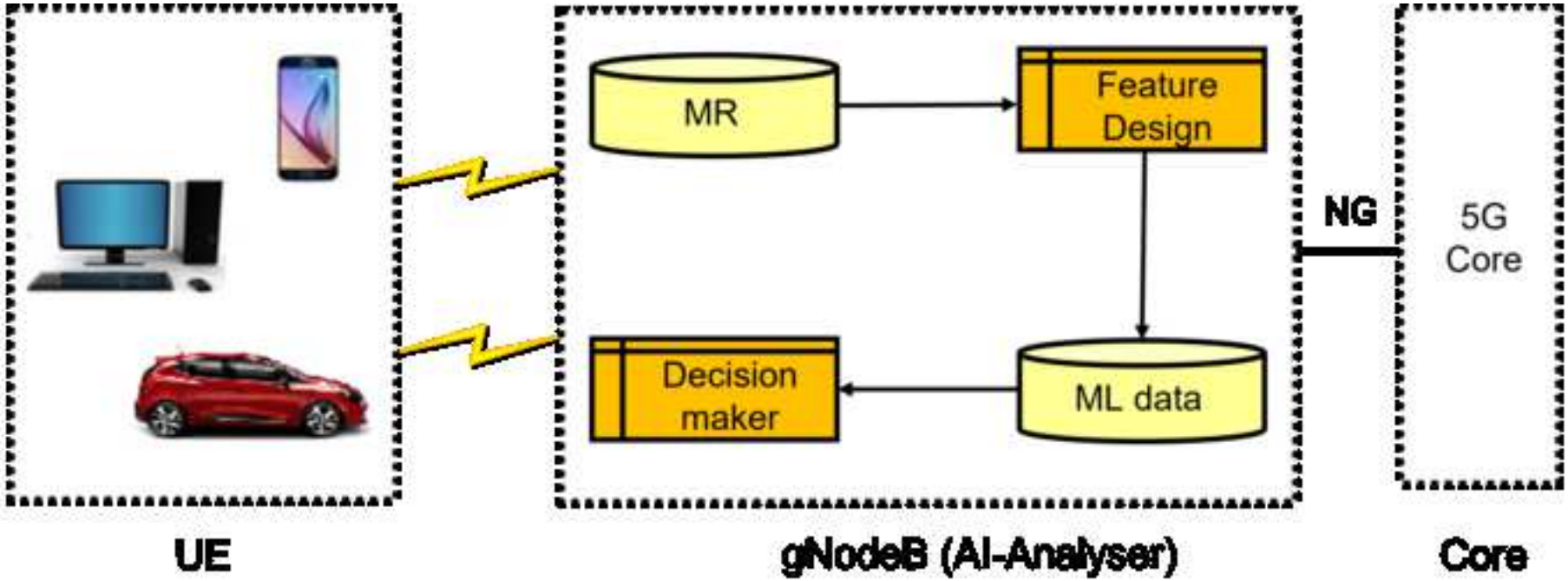

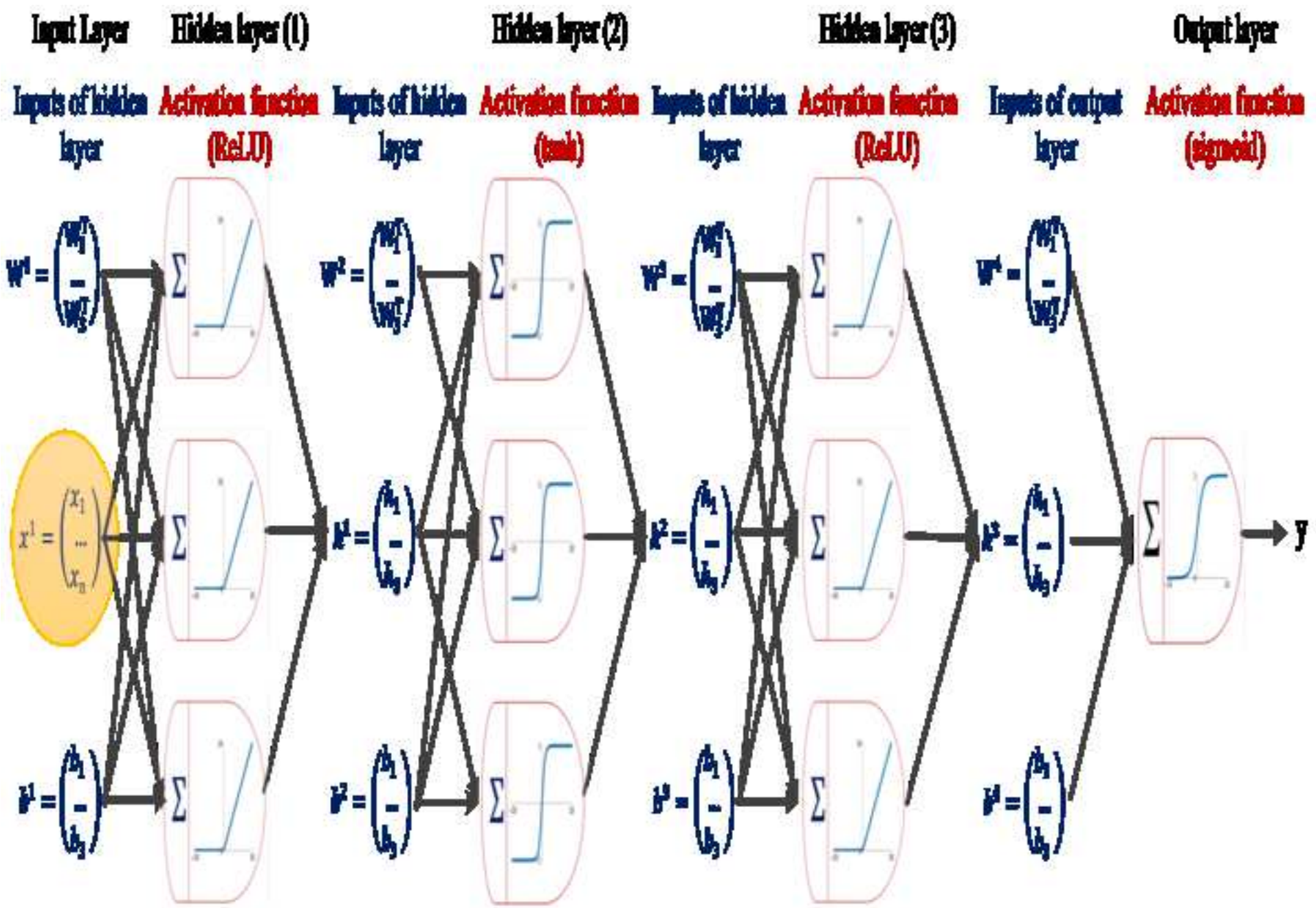

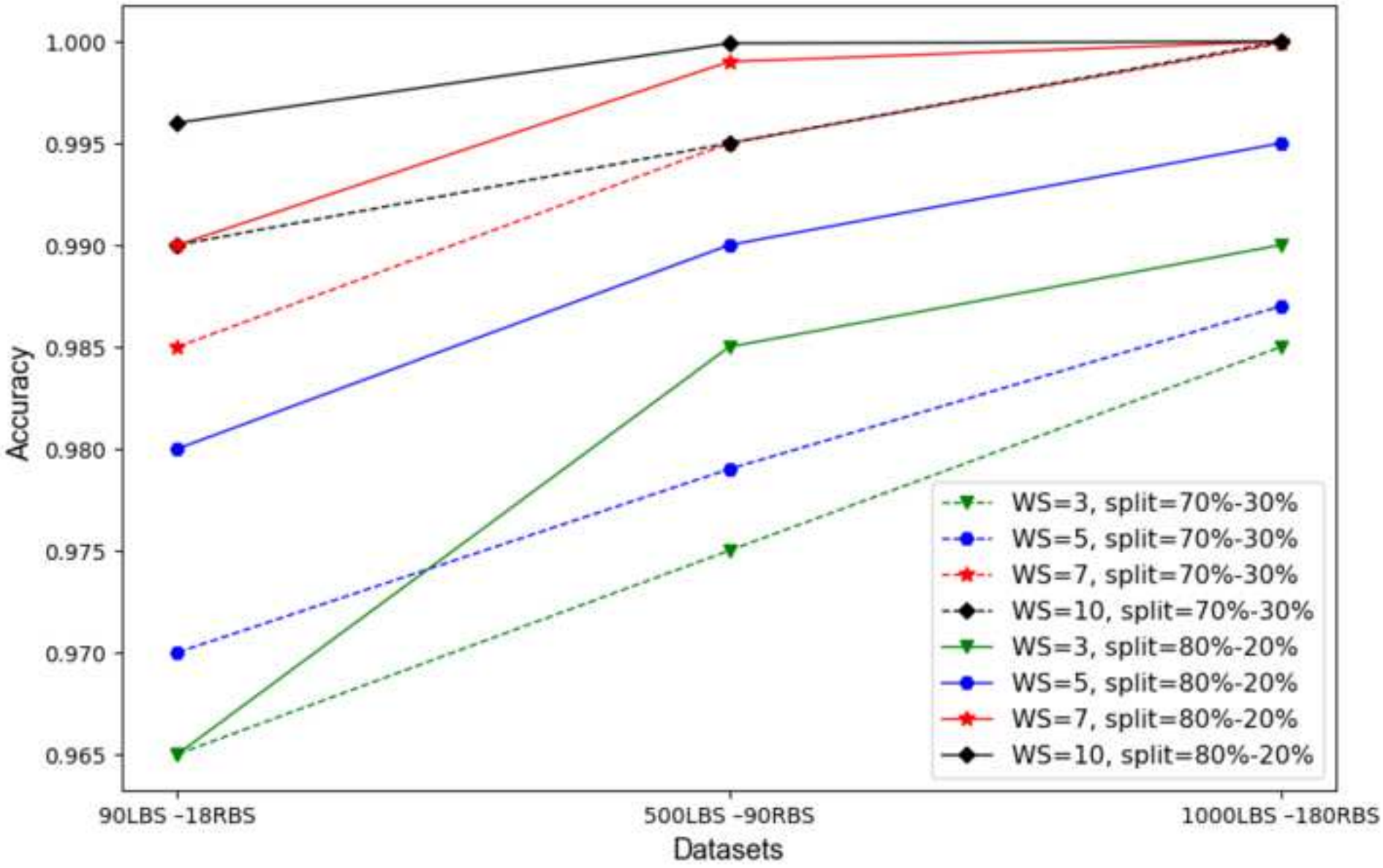

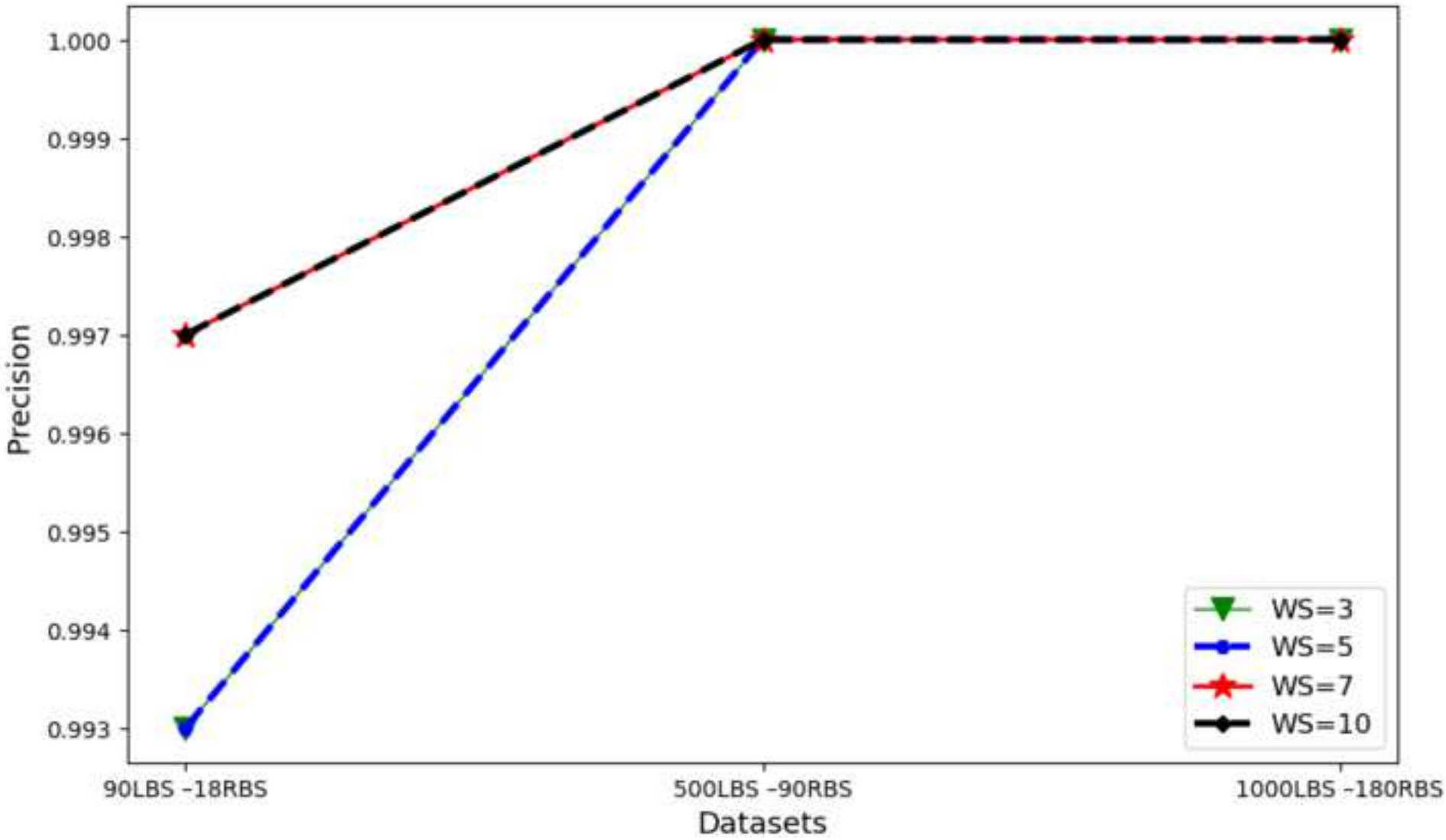

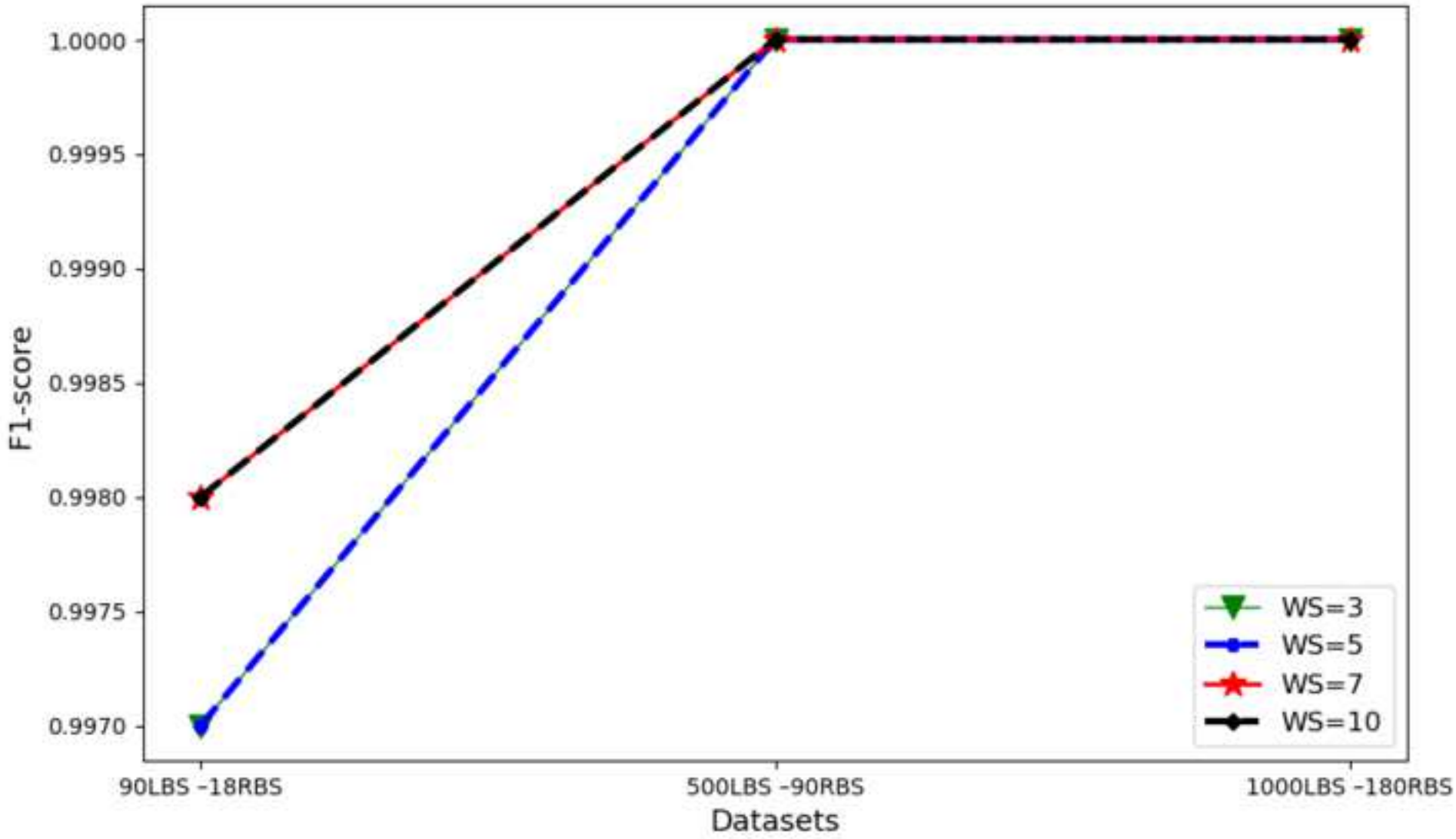

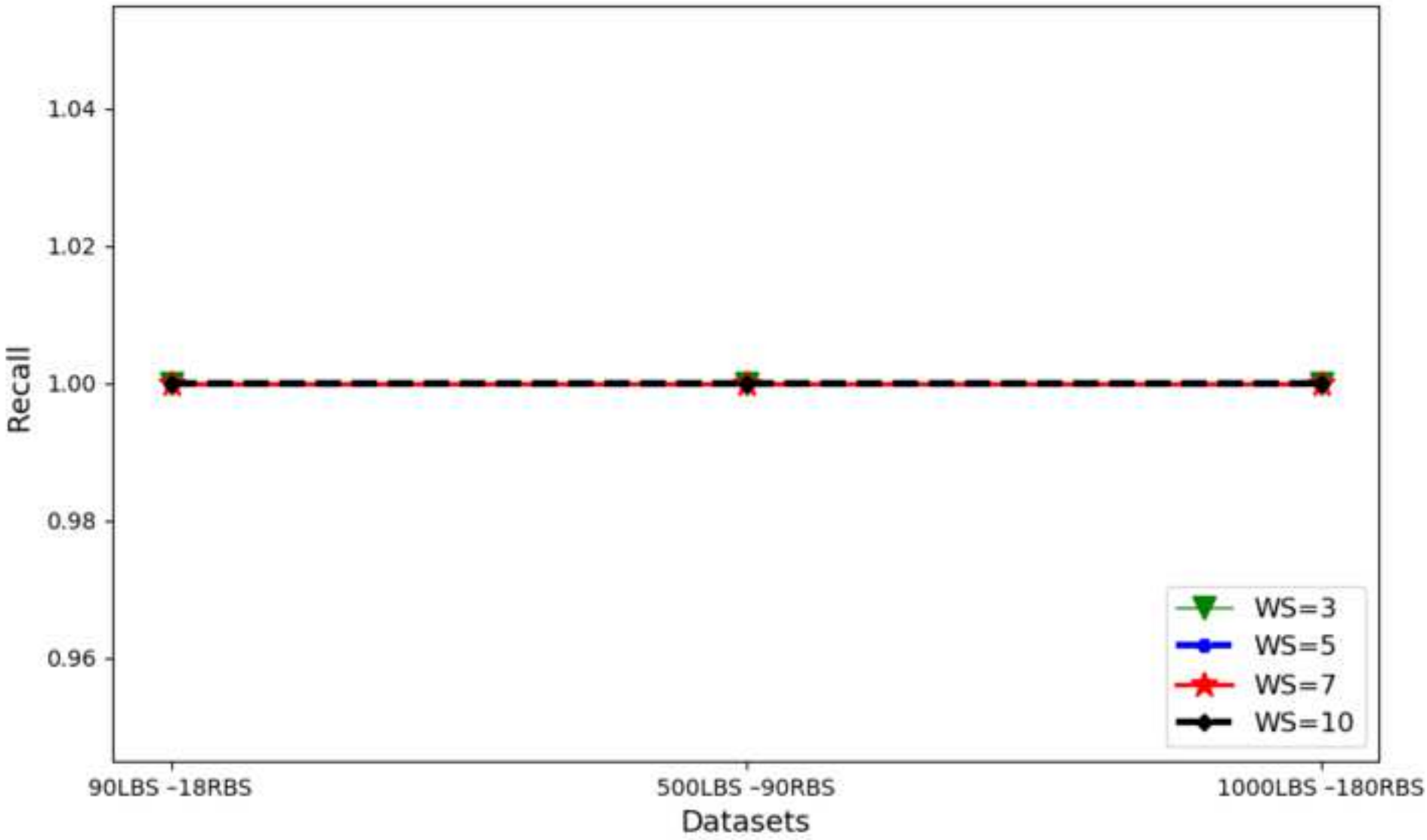

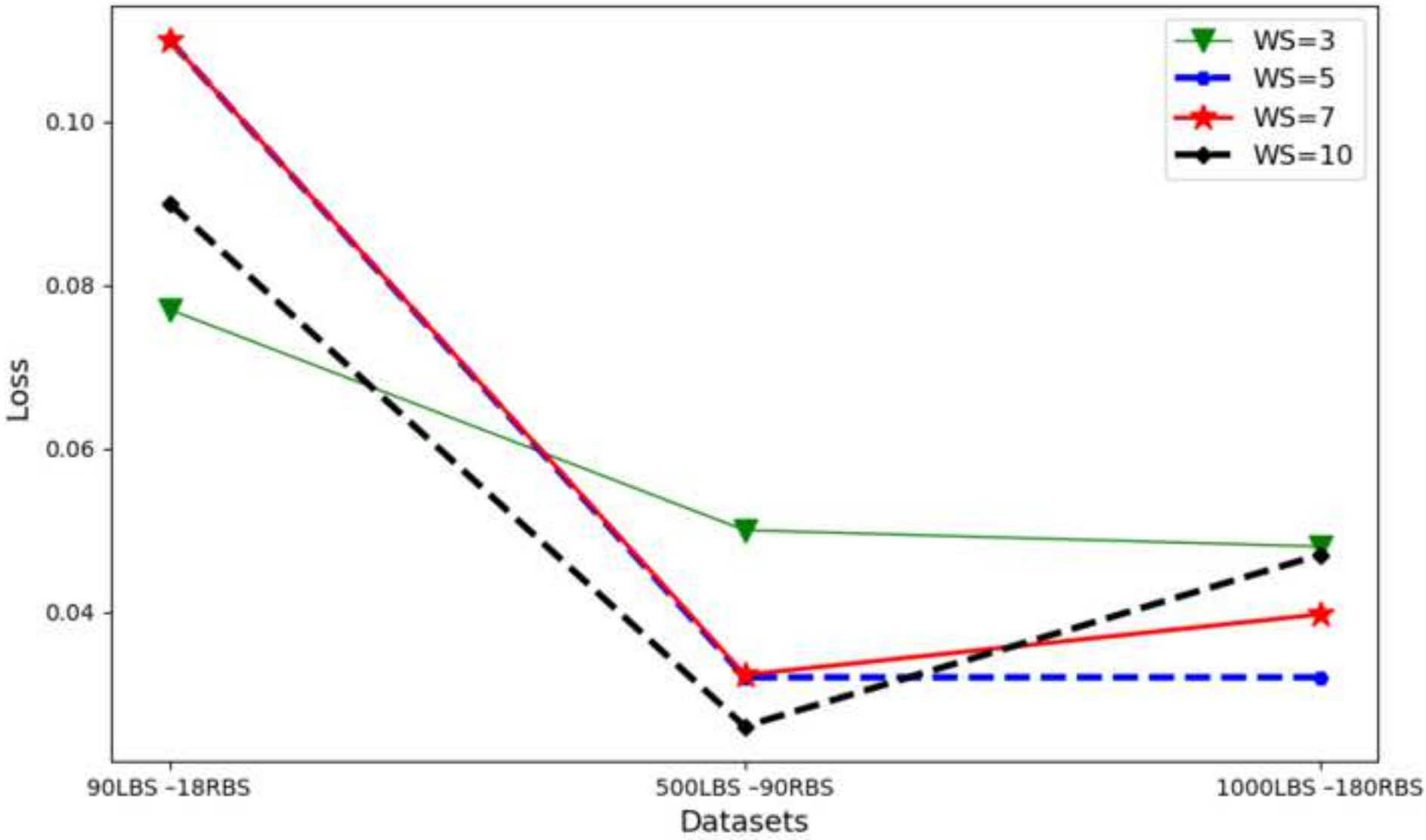

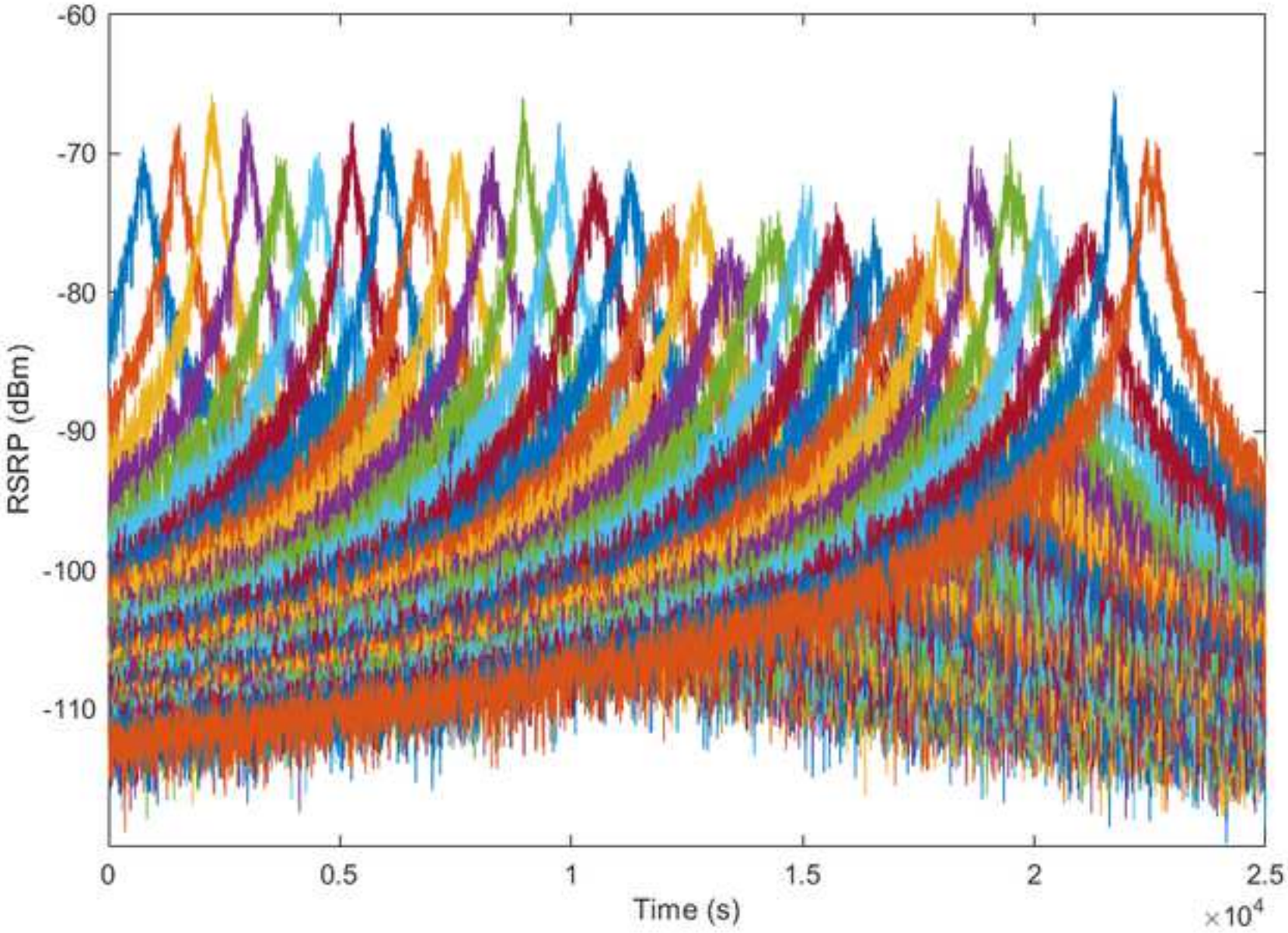

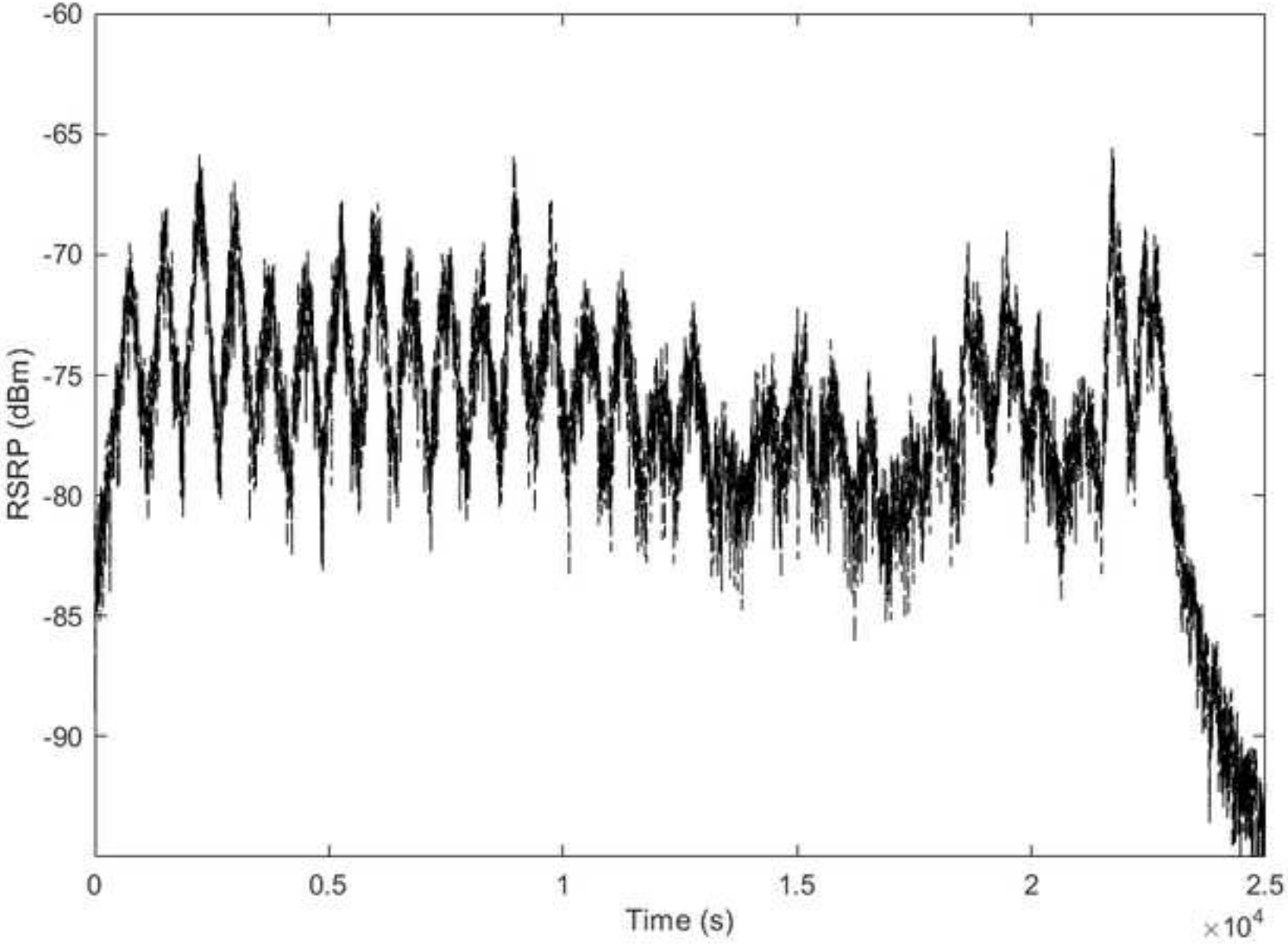

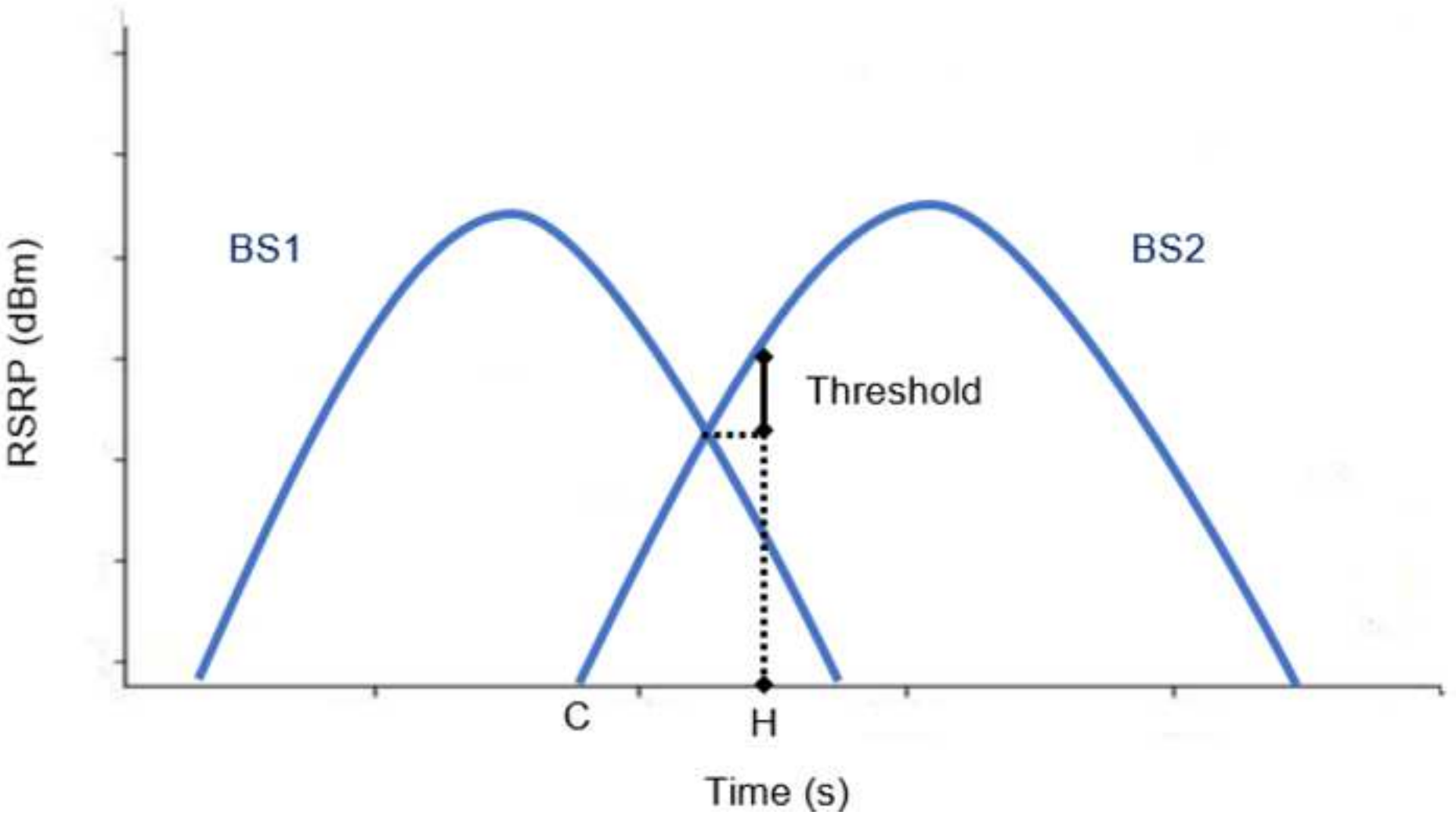

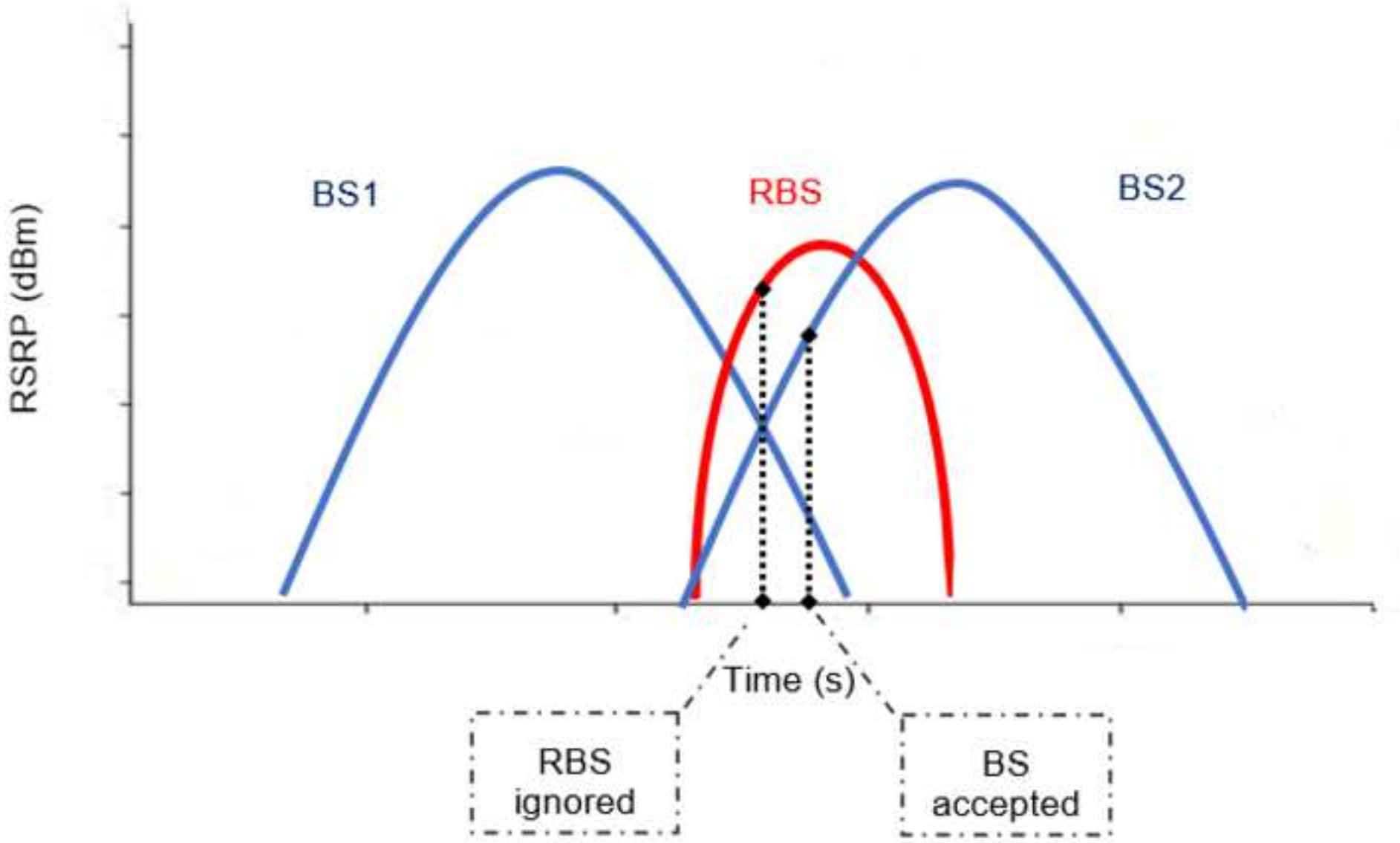

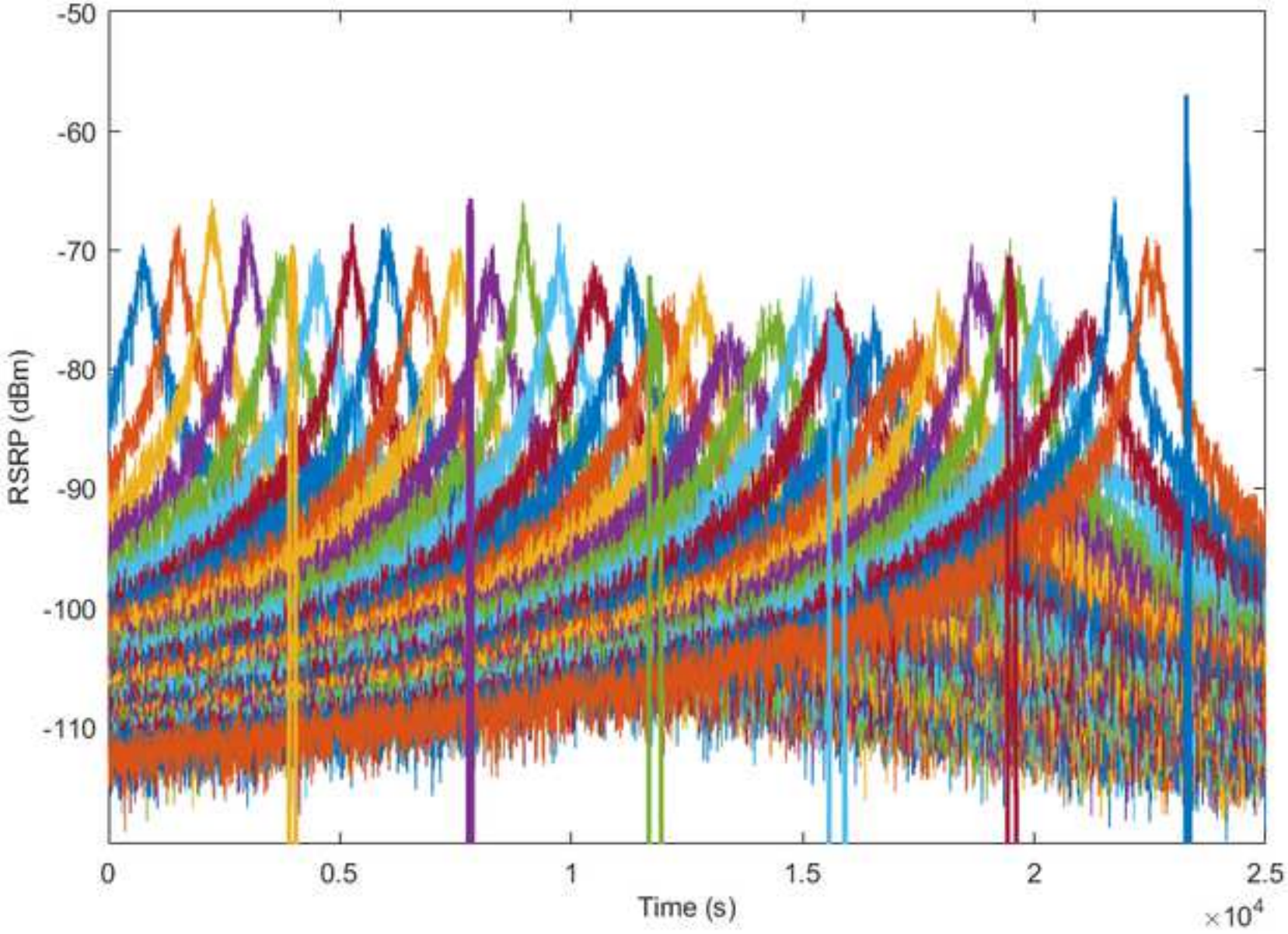

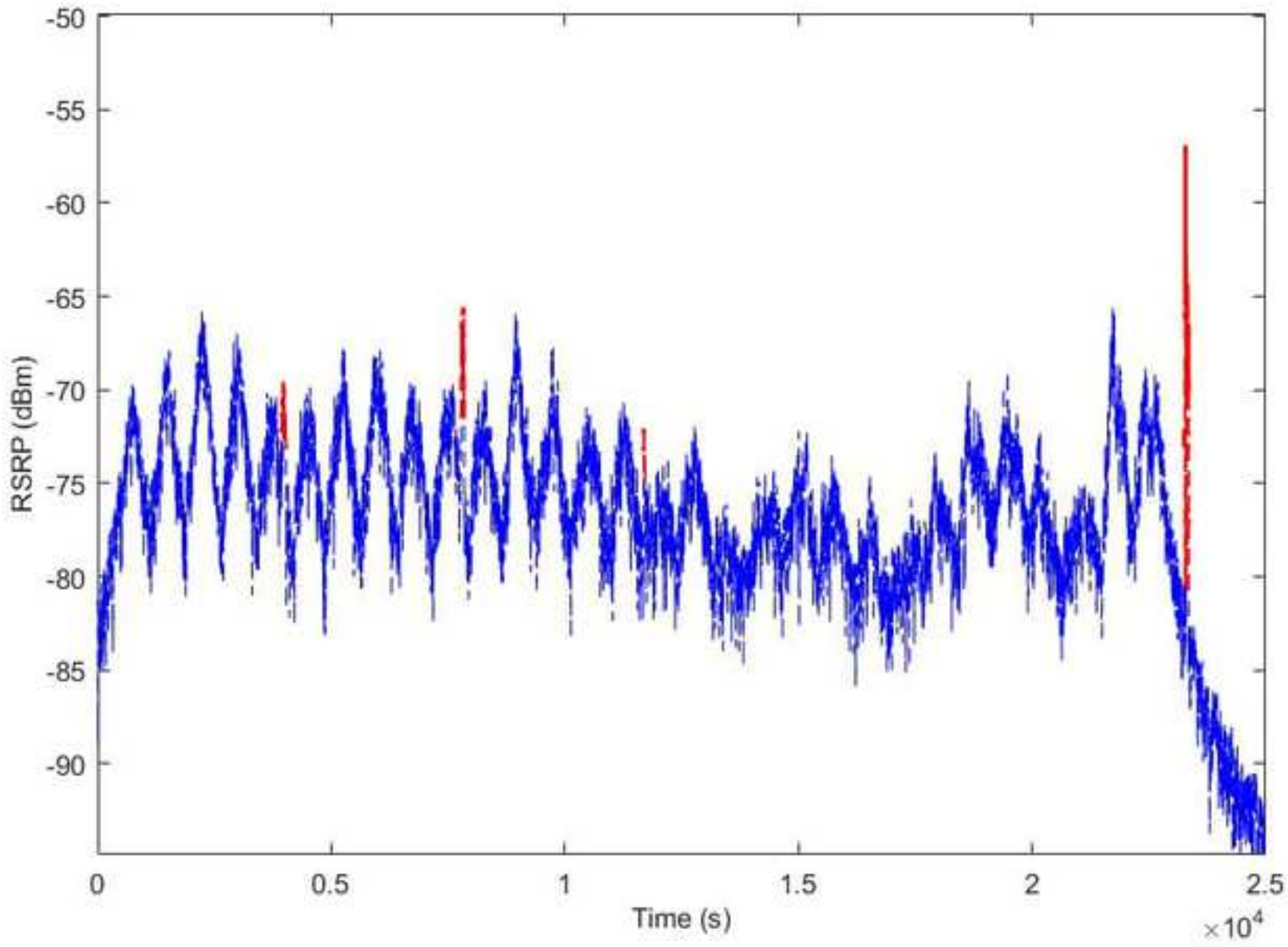

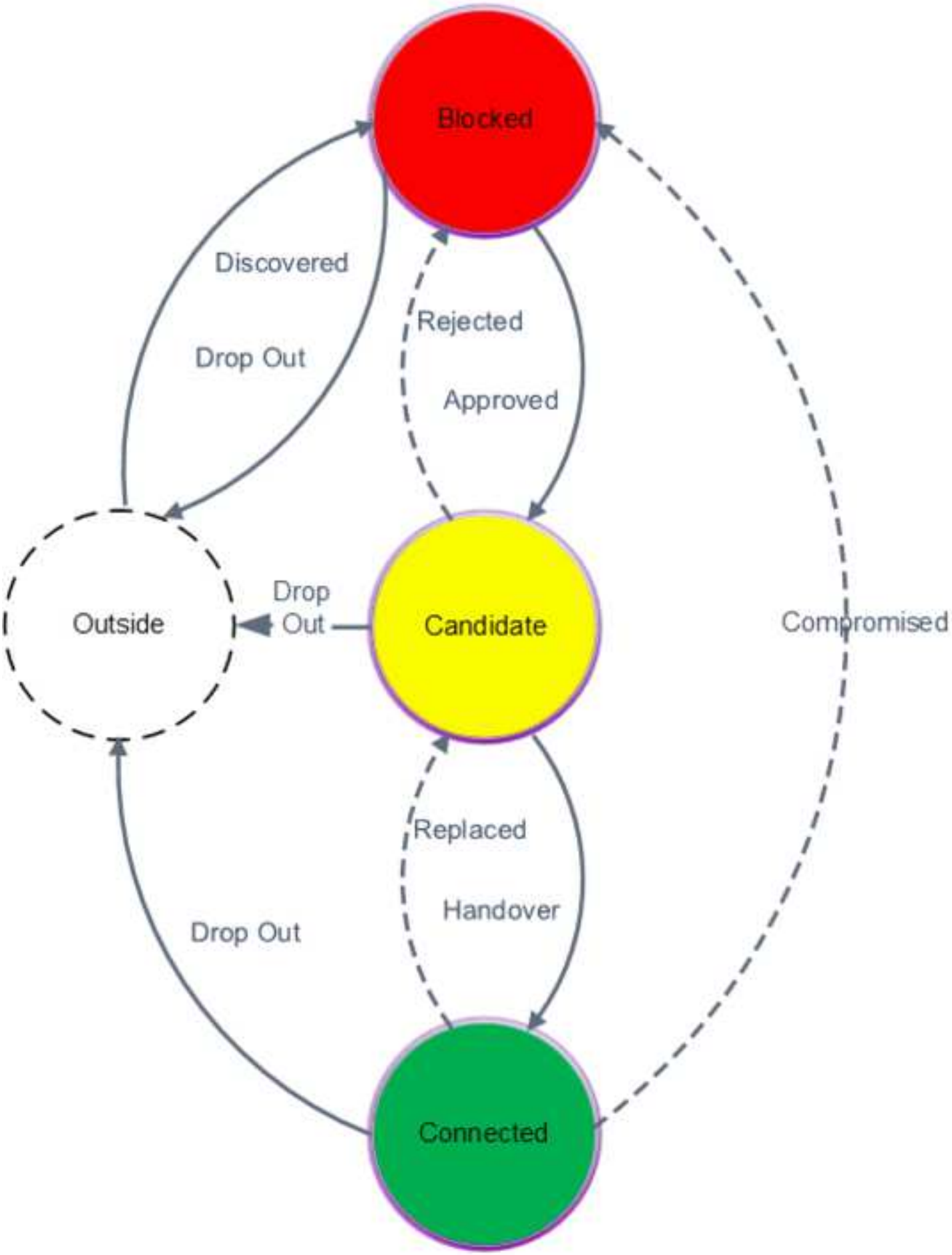

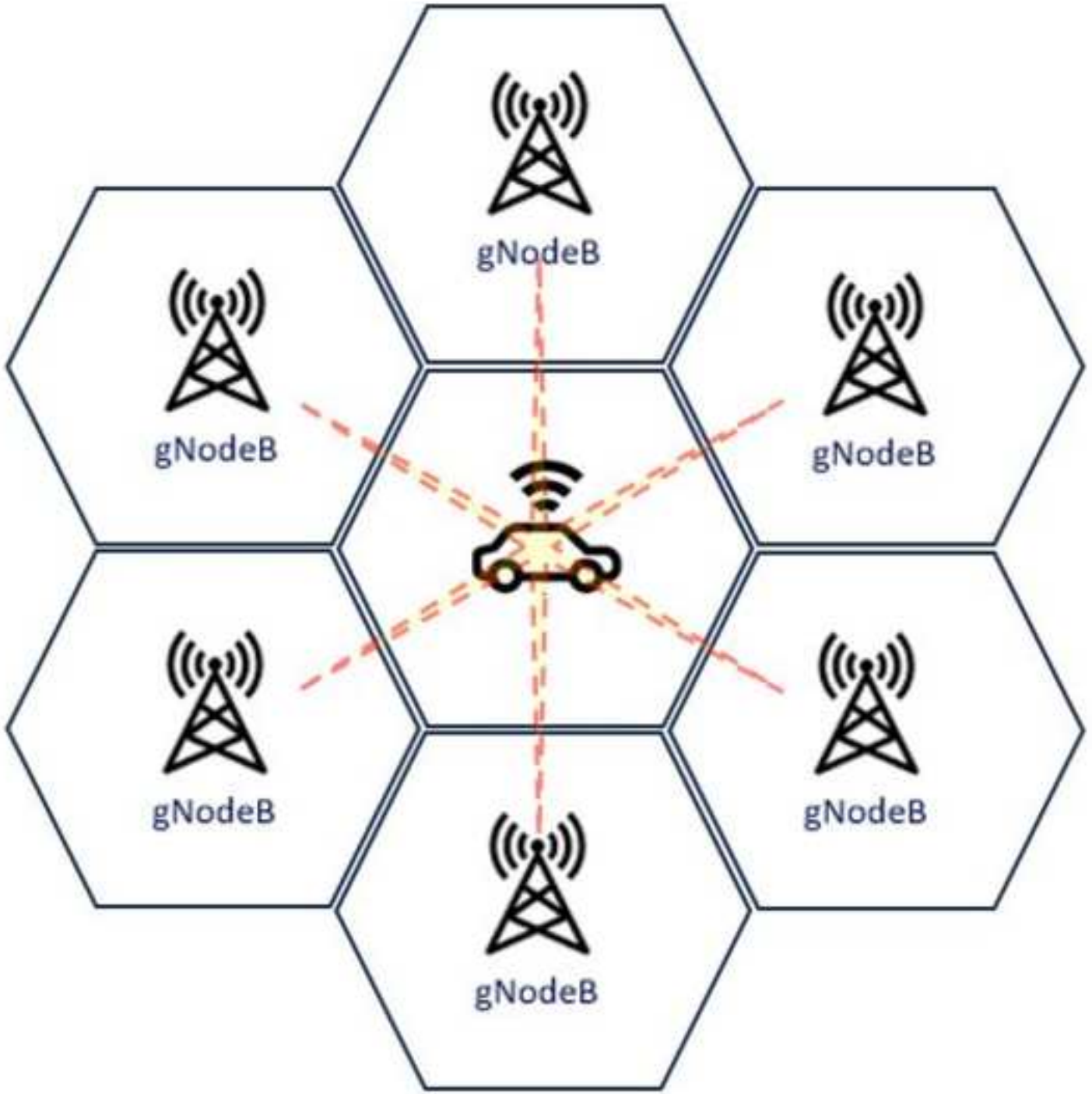

Declaration of interests

☒The authors declare that they have no known competing financial interests or personal relationships that could have appeared to influence the work reported in this paper.

☐The authors declare the following financial interests/personal relationships which may be considered as potential competing interests: